

1 Flood risk assessment for Indian sub-continental river basins

2 Urmin Vegad¹, Yadu Pokhrel², and Vimal Mishra^{1,3*}

3

4 ¹Civil Engineering, Indian Institute of Technology (IIT) Gandhinagar

5 ²Department of Civil and Environmental Engineering, Michigan State University, East Lansing, Michigan, USA

6 ³Earth Sciences, Indian Institute of Technology (IIT) Gandhinagar

7 *Corresponding author: vmishra@iitgn.ac.in

8 Abstract

9 Floods are among India's most frequently occurring natural disasters, which disrupt all aspects of socio-economic
10 well-being. A large population is affected by floods during almost every summer monsoon season in India, leaving
11 its footprint through human mortality, migration, and damage to agriculture and infrastructure. Despite the
12 massive imprints of floods, sub-basin level flood risk assessment is still in its infancy and requires advancements.
13 Using hydrological and hydrodynamical models, we reconstructed sub-basin level observed floods for the 1901-
14 2020 period. Our modelling framework includes the influence of 51 major reservoirs that affect flow variability
15 and flood inundation. Sub-basins in the Ganga and Brahmaputra River basins witnessed substantial flood
16 inundation extent during the worst flood in the observational record. Major floods in the sub-basins of the Ganga
17 and Brahmaputra occur during the late summer monsoon season (August-September). Beas, Brahmani, upper
18 Satluj, Upper Godavari, Middle and Lower Krishna, and Vashishti sub-basins are among the most influenced by
19 the dams, while Beas, Brahmani, Ravi, and Lower Satluj are among the most impacted by floods and the presence
20 of dams. Bhagirathi, Gandak, Kosi, lower Brahmaputra, and Ghaghara are India's sub-basins with the highest
21 flood risk. Our findings have implications for flood risk assessment and mitigation in India.

22 1. Introduction

23 Flood risk to both natural and human systems is projected to increase due to climate change (IPCC, 2014, 2022).
24 Extreme weather and climate extremes have increased under warming climate, leading to an increased frequency
25 of natural hazards like floods, droughts, heat waves, cyclones, and heavy rains. Hydroclimatic extremes affect
26 humans and infrastructure (Eidsvig et al., 2017; Peduzzi et al., 2009). Due to high vulnerability and lower adaptive
27 capacity, developing countries are often the most impacted by extreme weather events. Further, developing
28 countries usually take longer to recover from the hazards due to low climate resilience. Globally, floods are among
29 the most devastating natural hazards (Ghosh & Kar, 2018). Among all flood types, riverine floods occur most
30 frequently (Kimuli et al., 2021) and often cause substantial damage to agriculture and infrastructure. A
31 considerable fraction of the population and infrastructure are exposed to flooding, which will also increase due to
32 the projected increase in the magnitude and frequency of floods (Winsemius et al., 2018).

33 The increase in flood magnitude due to the warming climate has resulted in considerable economic losses (C. M.
34 R. Mateo et al., 2014; Willner et al., 2018). The total financial loss will likely increase by 17% in the next 20 years
35 due to climate change (Willner et al., 2018). Besides agriculture, floods significantly affect the built environment
36 and transportation infrastructure (Kalantari et al., 2014). For instance, more than 7% of road and railway assets

Formatted: Font: Times New Roman

Formatted: Font: Times New Roman, 10 pt

Formatted: Font: Times New Roman

Formatted: Font: Times New Roman

Formatted: Font: Times New Roman

Formatted: Font: Times New Roman

Formatted: Font: Times New Roman

Formatted: Font: Times New Roman

Formatted: Font: Times New Roman

Formatted: Font: Times New Roman

Formatted: Font: Times New Roman

Formatted: Font: Times New Roman, 10 pt

Formatted: Font: Times New Roman

Formatted: Font: Times New Roman

Formatted: Font: Times New Roman

Formatted: Font: Times New Roman

Formatted: Font: Times New Roman

Formatted: Font: Times New Roman

Formatted: Font: Times New Roman

Formatted: Font: Times New Roman

Formatted: Font: Times New Roman

Formatted: Font: Times New Roman

Formatted: Font: Times New Roman

Formatted: Font: Times New Roman

Formatted: Font: Times New Roman

Formatted: Font: Times New Roman

Formatted: Font: Times New Roman

Formatted: Font: Times New Roman

Formatted: Font: Times New Roman

Formatted: Font: Times New Roman

37 globally are exposed to a 100-year return period flood (Koks et al., 2019). In Asia, about 75% of the population
38 is exposed to riverine floods (Varis et al., 2022). India falls among the top ten most flood-affected countries in
39 Asia and the Pacific (Kimuli et al., 2021). In addition, India is also among the top-ten countries that experienced
40 the highest human mortality due to floods. Considerable population exposure, climate change, and rapid growth
41 and development in flood-prone areas contribute to increased losses from floods.

42 In India, state administration takes decisions to mitigate floods while the central government provides financial
43 aid under severe conditions (Jain et al., 2017). The state authorities develop action plans to minimize flood
44 damage. Therefore, identifying the regions with higher flood risk is essential for planning and mitigation. Flood
45 impacts can be quantified according to the affected population, gross domestic product (GDP), and agricultural
46 practices (Ward et al., 2013). The flood risk assessment framework suggested by the Intergovernmental Panel on
47 Climate Change (IPCC) has been extensively applied at the regional and global scales (Allen et al., 2016; IPCC,
48 2014; Roy et al., 2021). The risk can be quantified as a function of vulnerability, hazard, and exposure (IPCC,
49 2014). To control the risk, reducing vulnerability is considered a short to the mid-term goal (V. Mishra et al.,
50 2022), while reducing hazards and exposure are long-term goals (Birkmann & Welle, 2015). Flood risk assessment
51 can assist in identifying the regions at high risk due to higher vulnerability, hazard, and exposure, which can be
52 used for developing a framework, methodology, and guidelines for flood mitigation and damage assessment.

53 A flood risk assessment performed on a global scale may not help in identifying the flood risk-prone regions at a
54 country scale due to the coarser spatial resolution (Bernhofen et al., 2022). Due to complex geomorphological
55 characteristics and diverse climatic conditions, India is considered a relatively high flood-risk region (Hochrainer-
56 Stigler et al., 2021). Therefore, estimating flood risk on a finer scale (e.g. sub-basin level) is essential for reliable
57 flood risk assessment. There have been studies on regional or river basin scales (Allen et al., 2016; Ghosh & Kar,
58 2018; Roy et al., 2021); however, those do not provide flood risk at a sub-basin scale in India. In addition, the
59 impact assessment of floods on transport infrastructure (rail and road infrastructure) still needs to be improved in
60 the country (Pathak et al., 2020; P. Singh et al., 2018). In addition, the role of dams and reservoirs in the flood
61 risk assessment should be addressed (Hirabayashi et al., 2013; Yamazaki et al., 2018a). Dams and reservoirs
62 considerably influence streamflow variability and can attenuate flood peaks (Dang et al., 2019; Vu et al., 2022;
63 Zajac et al., 2017). In contrast, dam operations and decisions can also worsen the flood situation in the downstream
64 regions. For instance, recent flooding in Kerala and Chennai was partly attributed to reservoir operations (V.
65 Mishra & Shah, 2018). India has more than 5300 large dams regulating river flow (National Register of Large
66 Dams (NRLD), 2019), affecting ecosystems, natural resources, and livelihoods (Acreman, 2000). Reservoirs
67 impact flow regulation, magnitude, timing, and extent of flooding in the downstream regions. Therefore, flood
68 risk assessment without considering the role of reservoirs can be inappropriate in the basins that are highly affected
69 by the presence of dams.

70 We use the H08 (Hanasaki et al., 2018) global hydrological model combined with the CaMa-Flood (Yamazaki et
71 al., 2011) model for the sub-basin level flood risk assessment in India considering the role of reservoirs. The
72 CaMa-Flood model combined with the H08 model has been used for several river basins globally (Boulange et
73 al., 2021; C. M. R. Mateo et al., 2013). The CaMa-Flood model performs well in simulating flood dynamics
74 (Chaudhari and Pokhrel, 2022; H. Dang et al., 2022; Gaur & Gaur, 2018; Hirabayashi et al., 2013, 2021; Yamazaki
75 et al., 2018; Yang et al., 2019). The CaMa-Flood model takes runoff as input simulated from any hydrological

Formatted	... [1]
Formatted	... [2]
Formatted	... [3]
Formatted	... [4]
Formatted	... [5]
Formatted	... [6]
Formatted	... [7]
Formatted	... [8]
Formatted	... [9]
Formatted	... [10]
Formatted	... [11]
Formatted	... [12]
Formatted	... [13]
Formatted	... [14]
Formatted	... [15]
Formatted	... [16]
Formatted	... [17]
Formatted	... [18]
Formatted	... [19]
Formatted	... [20]
Formatted	... [21]
Formatted	... [22]
Formatted	... [23]
Formatted	... [24]
Formatted	... [25]
Formatted	... [26]
Formatted	... [27]
Deleted: 2018)	
Formatted	... [28]
Formatted	... [29]
Formatted	... [30]
Formatted	... [31]
Formatted	... [32]
Formatted	... [33]
Formatted	... [34]
Formatted	... [35]
Formatted	... [36]
Formatted	... [37]
Formatted	... [38]
Formatted	... [39]
Formatted	... [40]
Formatted	... [41]
Formatted	... [42]
Formatted	... [43]
Formatted	... [44]
Formatted	... [45]

80 model and can simulate flood depth and inundation. In India, almost all the major rivers are influenced by
81 reservoirs (Lehner et al., 2011). Therefore, the major scientific questions that we address are: 1) How does the
82 flood risk vary at the sub-basin level in India during the 1901-2020 period? 2) Which are the sub-basins where
83 the presence of reservoirs considerably influences the flood risk? To address these questions, we use long-term
84 observations (1901-2020) from India Meteorological Department (IMD) along with a hydrological modelling
85 framework.

86 2. Data and Methods

87 2.1 Datasets

88 We used observed gridded precipitation (Pai et al., 2014) and daily maximum and minimum temperatures
89 (Srivastava et al., 2009) from India Meteorological Department (IMD). We obtained gridded daily precipitation
90 at 0.25° from IMD for the 1901-2020 period that was developed using station-based rainfall observations from
91 more than 6900 gauge stations (Pai et al., 2014). The gridded rainfall product has been widely used for
92 hydrological studies (Kushwaha et al., 2021; Shah & Mishra, 2016) and it captures the key features of the summer
93 monsoon variability and orographic rainfall over the western Ghats and foothills of the Himalayas. We obtained
94 daily 1° gridded maximum and minimum temperatures from IMD (Srivastava et al., 2009). The gridded
95 temperature dataset is developed using observations from 395 stations located across India. Bilinear interpolation
96 was used to convert the 1° gridded temperature to 0.25° resolution to make it consistent with the gridded
97 precipitation. For the regions outside India, we obtained observational meteorological datasets (rainfall and
98 temperature) at 0.25 degrees from Princeton University (Sheffield et al., 2006). Gridded datasets from Sheffield
99 et al. (2006) compare well against the IMD observations and have been used in hydrological applications in India
100 (Shah & Mishra, 2016).

101 Observed daily streamflow at gauge stations and reservoir live storage were obtained from India Water Resources
102 Information System (India-WRIS). We considered the influence of 51 major reservoirs located in different river
103 basins to examine the impact of reservoirs on floods using the CaMa-Flood model (Figure S1). The information
104 of dams was obtained from the National Register of Large Dams (NRLD) [Table S1]. We used the Global Surface
105 Water (GSW) extent to estimate flood occurrences at a monthly timescale (Pekel et al., 2016). Simulated flood
106 occurrences during the period of the GSW database (1985-2020) were used to validate the performance of the
107 hydrological model in simulating flood extent (Pekel et al., 2016). In addition, we obtained reported flood details
108 from the Emergency Events Database (EM-DAT, <http://www.emdat.be/>) and Dartmouth Flood Observatory
109 (DFO, <http://floodobservatory.colorado.edu/>). EM-DAT is developed by the Centre for Research on the
110 Epidemiology of Disasters (CREED), while the University of Colorado manages DFO. We used population data
111 from Global Human Settlement Layers (GHLS) to estimate flood exposure. Finally, we used roadway and railway
112 network data to assess the impact of floods on the infrastructure.

113 2.2 H08-CaMa-Flood combined model

114 We used the H08 (Hanasaki et al., 2018) global hydrological model to simulate hydrological variables. The H08
115 is a distributed global water resources model comprising six sub-models: land surface hydrology, river routing,
116 reservoir operation, crop growth, environmental flow, and water abstraction. The model estimates baseflow using
117 a leaky bucket method, while runoff is calculated based on saturation excess non-linear flow (Hanasaki et al.,

Formatted	[... [46]
Formatted	[... [47]
Formatted	[... [48]
Formatted	[... [49]
Deleted: scale	
Formatted	[... [50]
Deleted: for the observed worst floods that occurred	
Formatted	[... [51]
Formatted	[... [52]
Formatted	[... [53]
Formatted	[... [54]
Formatted	[... [55]
Formatted	[... [56]
Formatted	[... [57]
Formatted	[... [58]
Formatted	[... [59]
Formatted	[... [60]
Formatted	[... [61]
Formatted	[... [62]
Formatted	[... [63]
Formatted	[... [64]
Formatted	[... [65]
Formatted	[... [66]
Formatted	[... [67]
Formatted	[... [68]
Formatted	[... [69]
Formatted	[... [70]
Formatted	[... [71]
Formatted	[... [72]
Formatted	[... [73]
Formatted	[... [74]
Formatted	[... [75]
Formatted	[... [76]
Formatted	[... [77]
Formatted	[... [78]
Formatted	[... [79]
Formatted	[... [80]
Formatted	[... [81]
Formatted	[... [82]
Formatted	[... [83]
Formatted	[... [84]
Formatted	[... [85]
Formatted	[... [86]
Formatted	[... [87]
Formatted	[... [88]
Formatted	[... [89]
Formatted	[... [90]

120 2008). The H08 model can be run separately or combined with any hydrodynamic model to perform flow routing.
121 The H08 model uses precipitation, air temperature, short and longwave radiations, wind speed, surface pressure,
122 and specific humidity as input meteorological forcing. Soil parameters for the H08 model were obtained from
123 Harmonized World Soil Database (HWSD). We forced the H08 model with the input meteorological forcing at
124 0.25° spatial and daily temporal resolution. We combined the H08 land surface model with the CaMa-Flood
125 model. The CaMa-Flood model has been previously combined with the H08 model to obtain flood inundation
126 estimates (C. M. Mateo et al., 2014).

Formatted: Font: Times New Roman

Formatted: Font: Times New Roman

127 The CaMa-Flood (version 4.1) is a hydrodynamic model (Yamazaki et al., 2011), which simulates river-floodplain
128 dynamics (Yamazaki et al., 2013). The CaMa-Flood model has been extensively used for better performance in
129 simulating discharge and flood peaks (Zhao et al., 2017). The CaMa-Flood model considers the role of dams and
130 reservoirs for streamflow and flood inundation simulations (Chaudhari & Pokhrel, 2022; C. M. Mateo et al., 2014;
131 Pokhrel et al., 2018). We ran the CaMa-Flood model at a finer spatial resolution (0.1°) using the H08-simulated
132 runoff (0.25°) as input. We calibrated the combined model (H08 and CaMa-Flood) for India's eighteen major river
133 basins for at least one gauge station each, considering the influence of 51 major dams. The gauge stations were
134 selected in the farthest downstream of the river basin based on the availability of observed streamflow. The
135 influence of reservoir operations was simulated using the CaMa-Flood model and evaluated against the observed
136 daily live reservoir storage.

Formatted: Font: Times New Roman

Formatted: Font: Times New Roman

Formatted: Font: Times New Roman

Formatted: Font: Times New Roman

Formatted: Font: Times New Roman

Formatted: Font: Times New Roman

Formatted: Font: Times New Roman

Formatted: Font: Times New Roman

Formatted: Font: Times New Roman

Formatted: Font: Times New Roman

Formatted: Font: Times New Roman

Formatted: Font: Times New Roman

Formatted: Font: Times New Roman

Formatted: Font: Times New Roman

Formatted: Font: Times New Roman

Formatted: Font: Times New Roman

Formatted: Font: Times New Roman

Formatted: Font: Times New Roman, 10 pt

Formatted: Font: Times New Roman

Formatted: Font: Times New Roman

Deleted: We manually calibrated the H08 model by adjusting four parameters

Formatted: Font: Times New Roman

Formatted: Font: Times New Roman, Font colour: Auto

Deleted:)

Deleted: .

Formatted: Font: Times New Roman

Formatted: Font: Times New Roman

Formatted: Font: Times New Roman

Formatted: Font: Times New Roman

Formatted: Font: Times New Roman

Formatted: Font: Times New Roman

Formatted: Font: Times New Roman

137 Large-scale global hydrological models do not perfectly capture the observed trends and variations as these are
138 often not well calibrated at river basin scale (Krysanova et al., 2018). The H08 model performs well when
139 calibrated at the river basin scale rather than coarser domains such as climate zones (Chuphal & Mishra, 2023;
140 Yoshida et al., 2022). Here, we manually calibrated the H08 model by adjusting four key parameters that
141 considerably influence streamflow, for each river basin, which include single-layer soil depth, gamma, bulk
142 transfer coefficient, and tau (Hanasaki et al., 2008; Raghav & Eldho, 2023). A more detailed discussion about the
143 calibration parameters of H08 are discussed in Dangar & Mishra (2021). Different sets of combinations of
144 calibration parameters within a range were used to calibrate the H08 model. The employed sets of parameters for
145 the 18 river basins in the Indian sub-continent are listed in Table S2. The calibrated parameters account for the
146 effect of human interventions because the model calibration is performed against the observed streamflow rather
147 than the naturalized streamflow (Duc Dang et al., 2020). We evaluated the model performance using the
148 coefficient of determination (R^2) and Nash-Sutcliffe Efficiency (NSE) for daily streamflow and reservoir live
149 storage. In addition, we compared the simulated and satellite-based observed flood occurrences. The satellite-
150 based flood occurrence is calculated using the Global Surface Water (GSW) dataset (Pekel et al., 2016), available
151 for the 1984-2020 period. We forced the well-calibrated combined (H08 and CaMa-Flood) models with observed
152 meteorological forcing from India Meteorological Department (IMD) at 0.25° spatial resolution to conduct
153 simulations from 1901 to 2020. The H08 model simulated runoff is used in CaMa-Flood to rout flood dynamics
154 at six arc-minutes (0.1 degrees). We generated the flood depth maps for the historical worst flood at the sub-basin
155 level. The worst flood is based on the highest magnitude of river flow observed at the subbasin outlet. The
156 generated flood depths at 6 arc-minutes (0.1°) were further downscaled to 1 arc-minute (~0.185 km) resolution
157 using the downscaling module available within the CaMa-Flood.

163 We used C-ratio (Nilsson et al., 2005; Zajac et al., 2017) to assess the potential impact of dams along a river. The
164 C-ratio is an identifier calculated as the ratio of total maximum storage capacity of the upstream reservoirs to the
165 mean annual discharge at a gauge station in the downstream region (Nilsson et al., 2005; Zajac et al., 2017). We
166 calculated the C-ratio at the outlets of each sub-basins that are influenced by the presence of dams. A C-ratio of
167 less than 0.5 indicates that the sub-basin is minimally affected by the presence of dams. Further, to identify sub-
168 basins susceptible to flood inundation resulting from dam operations, we multiplied the percentage of flooded
169 area in each sub-basin by its corresponding C-ratio. This enabled us to identify the sub-basins that experience
170 substantial flood inundation and are considerably impacted by the presence of reservoirs. Finally, we estimated
171 the exposed rail and road infrastructure affected by floods. The flooded area overlapped over the road and railway
172 network to estimate the network length affected by floods in a sub-basin. We considered the flooded area of the
173 observed worst flood. The subbasins with the highest rail and road infrastructure exposure to floods were
174 identified.

- Formatted: Font: Times New Roman
- Formatted: Font: Times New Roman
- Formatted: Font: Times New Roman
- Formatted: Font: Times New Roman
- Formatted: Font: Times New Roman
- Formatted: Font: Times New Roman
- Formatted: Font: Times New Roman

175 2.3 Risk assessment

176 We estimated flood risk using hazard, exposure, and vulnerability based on the common framework adopted by
177 the United Nations in the Global Assessment Reports of the United Nations Office for Disaster Risk Reduction
178 (UNISDR, 2011, 2013). A similar framework was used in previous studies for flood risk assessments (C. M. R.
179 Mateo et al., 2014; Tanoue, 2020; Winsemius et al., 2013). We multiplied the normalized values of hazard,
180 exposure, and vulnerability to estimate the risk as:

- Formatted: Font: Times New Roman
- Formatted: Font: Times New Roman
- Formatted: Font: Times New Roman
- Formatted: Font: Times New Roman
- Formatted: Font: Times New Roman
- Formatted: Font: Times New Roman
- Formatted: Font: Times New Roman

$$181 \text{ Risk} = \text{Vulnerability} * \text{Exposure} * \text{Hazard} \dots \dots (1)$$

182 The flood risk assessment can help identify the hotspots and prioritize climate adaptation (de Moel et al., 2015).
183 Among the three components, vulnerability is a degree of damage to a particular object at flood risk with a
184 specified amount and present on a scale from 0 to 1. We obtained the vulnerability index for each district from
185 the "Climate Vulnerability Assessment for Adaptation Planning in India Using a Common Framework", a report
186 developed by the Department of Science and Technology
187 (<https://dst.gov.in/sites/default/files/Ful%20Report%20%281%29.pdf>). The vulnerability of each district is
188 calculated using 14 indicators, each with equal weights. The indicators capture both sensitivity and adaptive
189 capacity. We estimated the vulnerability index of each sub-basin by taking the spatial mean of the vulnerability
190 of the districts falling into the sub-basins. Exposure is termed as assets and population in a flood-exposed area
191 resulting in flood damage (Marchand et al., 2022). The population dataset is a critical component in performing
192 exposure estimation. The exposure is defined as the fraction of the population exposed to the flood extent (Smith
193 et al., 2019). We completed the flood exposure estimate using the Global Human Settlement Layers (GHSL)
194 population dataset (Joint Research Centre (JRC) et al., 2021), which is available at a resolution of 30 arc-seconds
195 for 1975, 1990, 2000, 2014 and 2015. We used the population data for the year 2015 throughout this study. We
196 rescaled the population data to 6 arc-minutes to make it consistent with the flooded area simulated from the
197 combined model. We estimated the hazard as the exceedance probability of a flooded area exceeding half of the
198 historical maximum flooded area in the last 50 years. We used normalized vulnerability, exposure, and hazard to
199 estimate the risk.

- Formatted: Font: Times New Roman
- Formatted: Font: Times New Roman
- Formatted: Font: Times New Roman
- Formatted: Font: Times New Roman
- Formatted: Font: Times New Roman
- Formatted: Font: Times New Roman
- Formatted: Font: Times New Roman
- Formatted: Font: Times New Roman
- Formatted: Font: Times New Roman
- Formatted: Font: Times New Roman
- Formatted: Font: Times New Roman
- Formatted: Font: Times New Roman
- Formatted: Font: Times New Roman
- Formatted: Font: Times New Roman
- Formatted: Font: Times New Roman
- Formatted: Font: Times New Roman
- Formatted: Font: Times New Roman
- Formatted: Font: Times New Roman
- Formatted: Font: Times New Roman
- Formatted: Font: Times New Roman

200 3. Results

201 3.1 Calibration and evaluation of hydrological models

202 We calibrated and evaluated the performance of the H08 and CaMa-Flood combined models against the observed
203 daily streamflow (Figure 1). Due to the unavailability of daily observed streamflow for the three transboundary
204 river basins (Indus, Ganga and Brahmaputra), we used observed monthly streamflow to calibrate the model. In
205 addition, we evaluated the model performance for daily live storage of the 51 reservoirs after the calibration
206 against the observed flow (Figure 1). The model exhibited good skills ($R^2 > 0.6$ and $NSE > 0.6$) for almost all the
207 river basins except Cauvery, East Coast, Northeast Coast, and Sabarmati. The model also performed well with
208 NSE greater than 0.6 for more than 80% of the selected reservoirs in simulating daily live storage for the selected
209 reservoirs. We estimated the bias and timing error in simulating peak discharge at all the selected gauge stations
210 (Figure S2). We calculated the bias in the model simulated annual maximum streamflow against the observed
211 annual maximum streamflow for the time periods for which observations are available. We excluded the
212 transboundary rivers (Ganga, Brahmaputra and Indus) as timing error (in days) could not be estimated due to the
213 unavailability of daily observed flow. While other gauge stations exhibited moderate bias, gauge stations in
214 Cauvery, Sabarmati, and Mahi rivers basins show a considerable dry bias. Contrary to several other stations where
215 the mean timing error was below two days, the Sabarmati river basin displayed a comparatively higher mean
216 timing error. The relatively poor performance of the model in these river basins can be attributed to the lack of
217 long-term observations as well as substantial human interventions that can affect the observed flow.

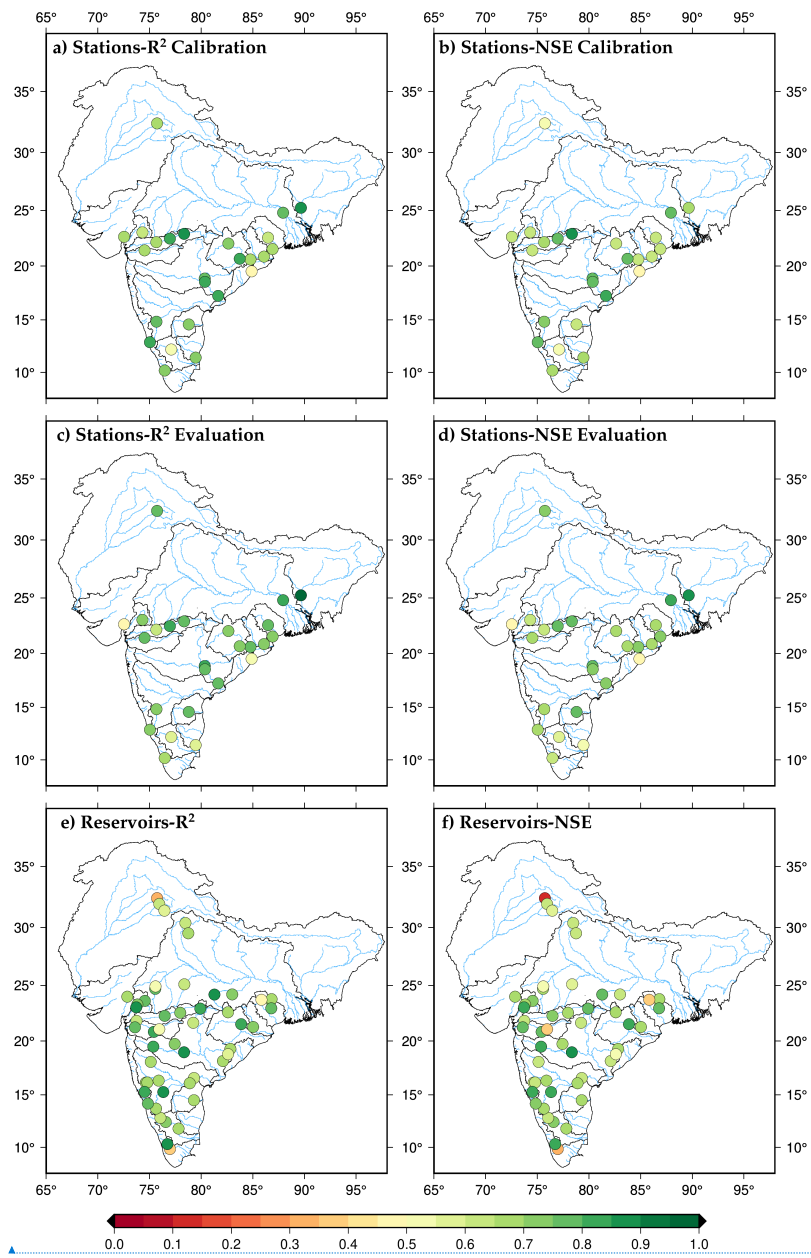
218 We compared model-simulated, and satellite-based observed flood occurrence for the 1984-2020 period (Figure
219 2). In addition, we compared the model-simulated flood events against Sentinel-1 SAR and MODIS satellite-
220 based imagery for a few flood events based on the satellite data availability (Figures. 3, S3, S4). We found that
221 the model simulated flood extent captures the satellite based flood extent. However, we note that the model
222 overestimated the flood extent in Ganga river basin and underestimated in Brahmaputra river basin, therefore,
223 showing a non-systematic bias. Moreover, a considerable difference in the flood extent based on the two satellite
224 datasets was observed, which highlights the observational uncertainty in the estimation of flood extent. In general,
225 the model exhibits satisfactory performance in simulating flood extent against the satellite-based observations.
226 However, the model overestimates flood extent in the Ganga basin, which could be attributed to the influence of
227 cloud contamination and dense vegetation cover on satellite-based flood estimates (Chaudhari & Pokhrel, 2022).
228 On the other hand, the model underestimates the flood occurrence in the upstream region of the Brahmaputra
229 River. This could be due to limitations in model parameterization, as observed flow is limited in the transboundary
230 river basins. Despite the good performance against the observed streamflow, the simulated flood extent has a
231 considerable bias, which can be attributed to satellite-based flood extent mapping limitations and the model's
232 ability to capture the flood extent accurately. The model-simulated flood extent shows a good agreement against
233 the reported flood from EM-DAT and DFO databases (Figure S5). In addition, the simulated flood extent also
234 showed a good agreement with the reported flood in cities in the Brahmaputra and Ganga River basins. Given the
235 limitation in the streamflow and flood extent observations, the hydrological models perform satisfactorily and can
236 be used for the sub-basin level risk assessment.

Formatted: Font: Times New Roman

Formatted: Font: Times New Roman, 10 pt

Formatted: Font: Times New Roman

Formatted: Font: Times New Roman



Formatted: Font: Times New Roman

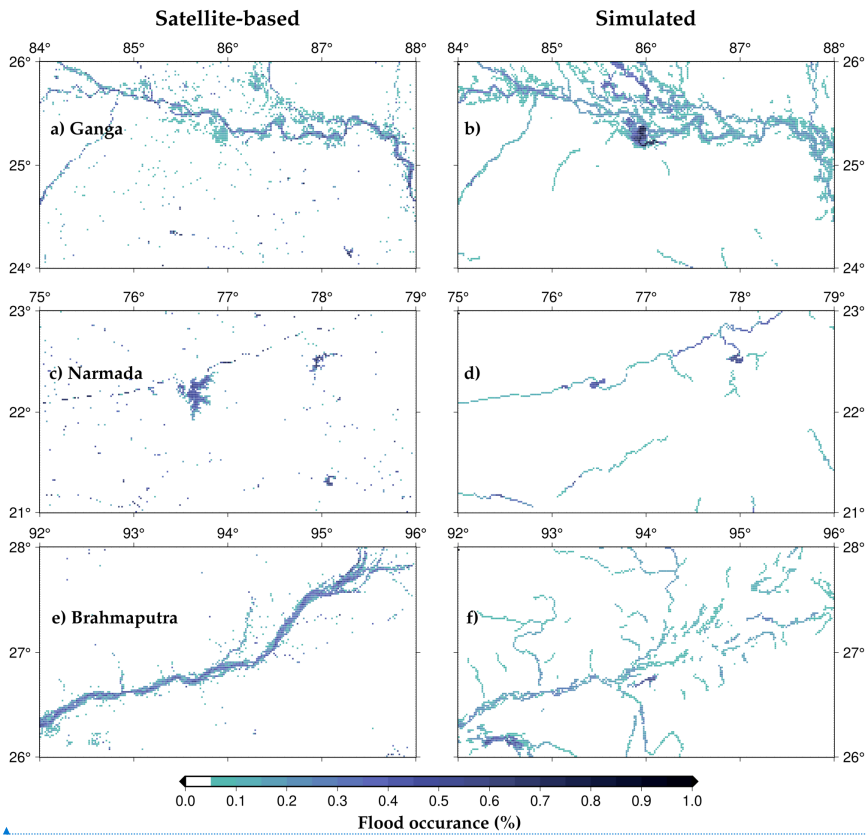
Formatted: Font: Times New Roman

237

238 Figure 1: Calibration and evaluation of the combined model for daily river flow and reservoir storage at
 239 gauge stations and daily live storage of reservoirs

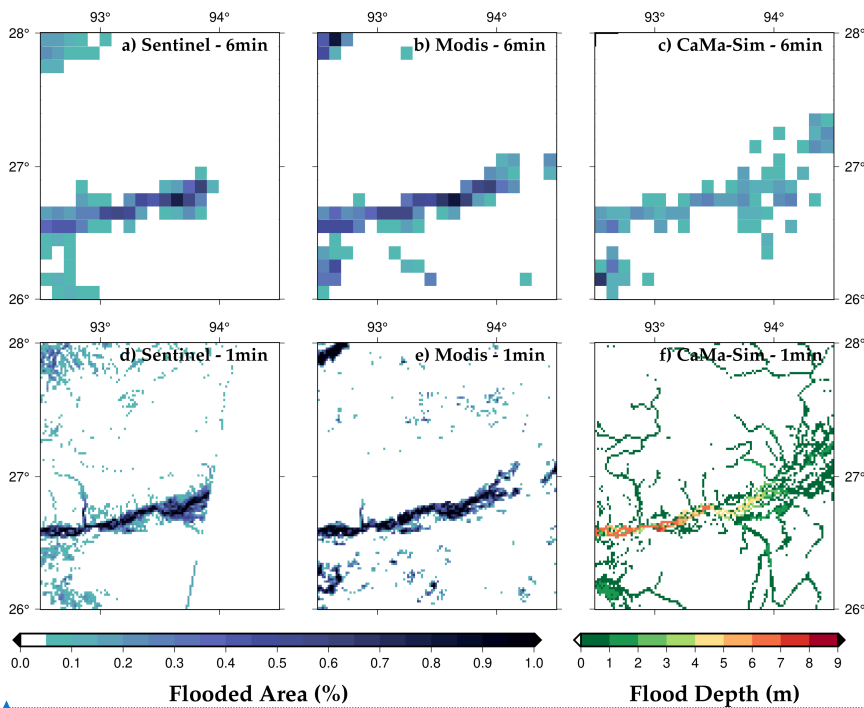
Formatted: Font: Times New Roman

Formatted: Font: Times New Roman



240

241 **Figure 2: Simulated flood occurrences compared with satellite-based flood occurrence for different**
242 **regions in Ganga, Narmada and Brahmaputra River basin.**



Formatted: Font: Times New Roman

Formatted: Font: Times New Roman

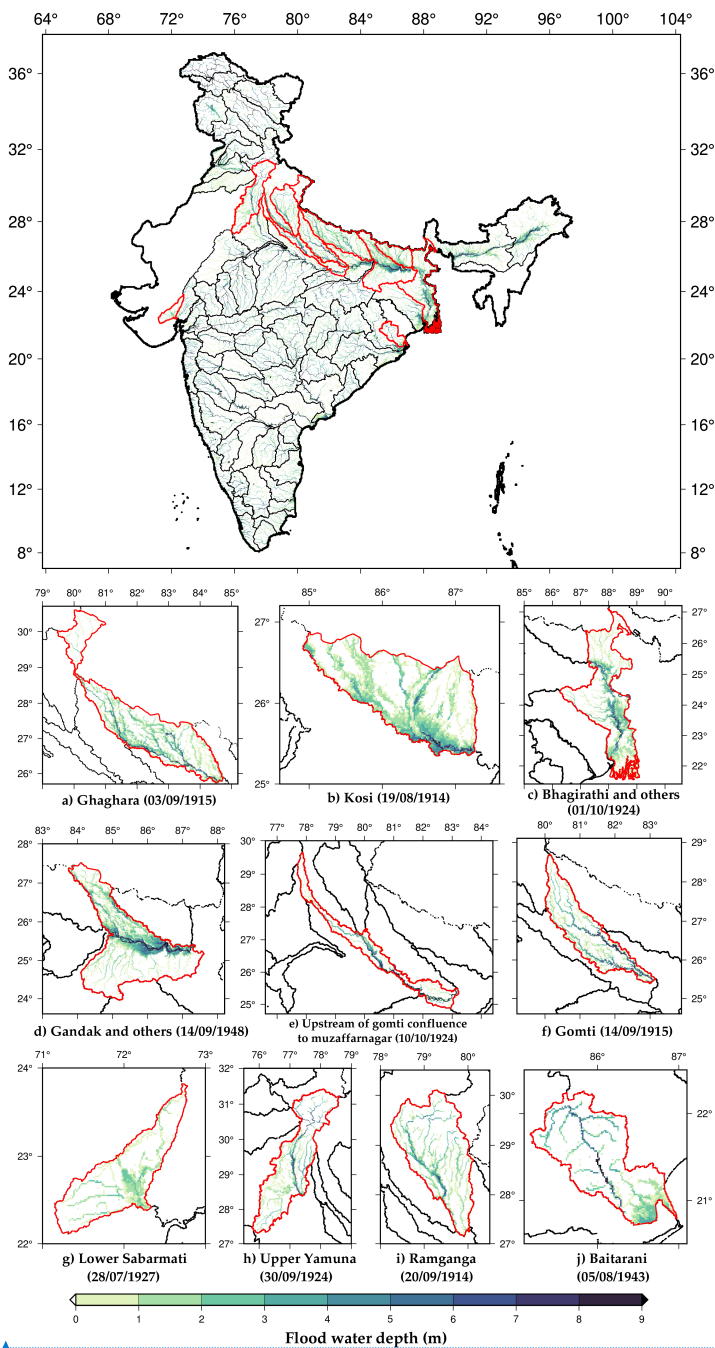
243 **Flooded Area (%)** **Flood Depth (m)**

244 **Figure 3: Simulated flood extent compared with Sentinel-1 SAR and MODIS satellite-based flood extent**
 245 **for the 2016 flood event in the Brahmaputra river**

246 **3.2 Estimation of the observed flood extent**

247 Next, we reconstructed the flood inundation for the observed worst flood for each sub-basin for the 1901-2020
 248 period in India. The inundation extent for the worst flood can help us identify the sub-basin with higher flood risk.
 249 We estimated flood depth and inundated area for each sub-basin for the worst flood during the last 120 years
 250 (Figure 4). In addition, we identified the occurrence of the worst flood at the sub-basin level during the 1901-2020
 251 period. We highlighted ten sub-basins that experienced the highest fractional area affected by the worst flood.
 252 Sub-basins in the Ganga and Brahmaputra rivers are among the most highly influenced by the worst flood. For
 253 instance, Ghaghra, Kosi, Bhagirathi, Gandak, Gomti, lower Sabarmati, upper Yamuna, Ramganga, and Baitarani
 254 sub-basins had the highest fractional area affected by the worst flood during 1901-2020 (Figure 4). The fractional
 255 area of sub-basins in the semi-arid western India is less affected compared to those located in the Ganga basin.
 256 For example, the lower Sabarmati sub-basin of the Sabarmati River basin is among the sub-basins that are highly
 257 influenced by the observed worst flood. We also find that the worst flood in the same year did not affect all the
 258 sub-basins within a river basin (Figure S6). For instance, all the highly influenced sub-basins experienced the
 259 worst flood in different years in the Ganga basin (Figure 4). Most of the top flood-affected sub-basins experienced
 260 floods during August-September in the summer monsoon season. Overall, the flood extent due to the worst flood

261 is substantially greater in the sub-basins of the Ganga and Brahmaputra river basins compared to other basins in
262 India (Figure 4). Ganga river basin also has the highest population density among all the basins in the Indian sub-
263 continent, which makes it vulnerable for the flood risk.



Formatted: Font: Times New Roman

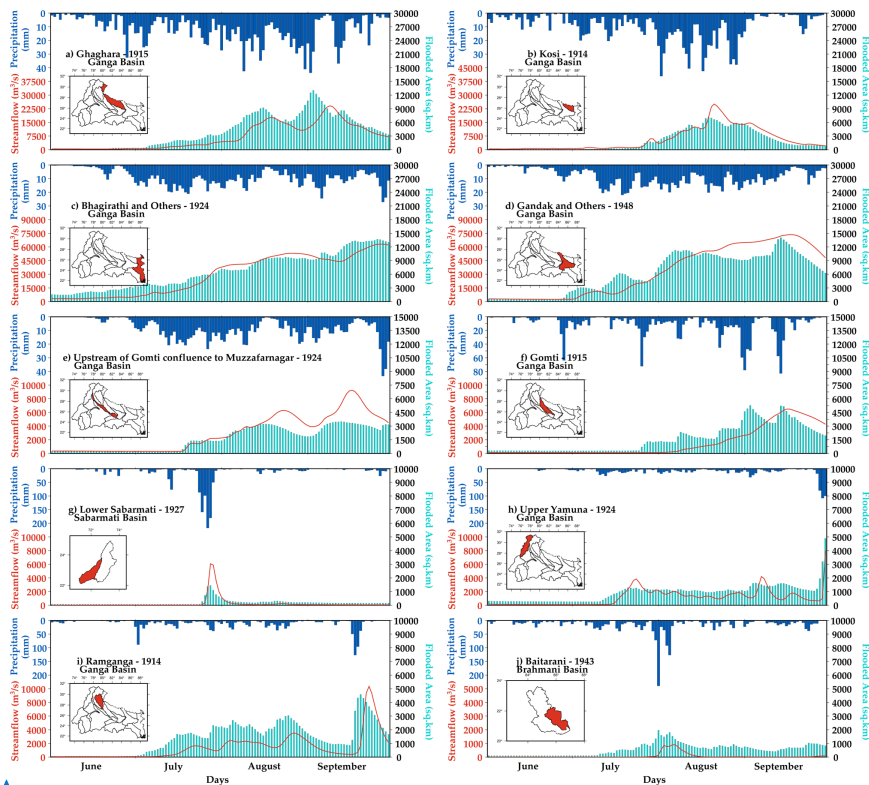
Formatted: Font: Times New Roman

265 **Figure 4: Flood depth map for the observed worst flood for each sub-basins, highlighting the sub-basins**
266 **with maximum flood inundated area (%) (a) Ghaghara – Ganga River basin (b) Kosi – Ganga River basin**
267 **(c) Bhagirathi and others – Ganga River basin (d) Gandak and others – Ganga River basin (e) Upstream**
268 **of Gomti confluence to Muzaffarnagar – Ganga River basin (f) Gomti – Ganga River basin (g) Lower**
269 **Sabarmati – Sabarmati River basin (h) Upper Yamuna – Ganga River basin (i) Ramganga – Ganga River**
270 **basin (j) Baitarani – Brahmani River basin**

271 Next, we examined the precipitation, streamflow, and flood-affected area (%) for the ten sub-basins that had the
272 highest fractional flood affected area for the worst flood during 1901-2020 (Figure 5). As floods mostly occur
273 during the summer monsoon season in India (V. Mishra et al., 2022; Nanditha & Mishra, 2021), we examined the
274 temporal variability of precipitation, and streamflow during the monsoon season of the worst flood year. Nanditha
275 and Mishra (2022) reported that multi-day precipitation is India's most robust driver of floods. Moreover, extreme
276 precipitation and wet-antecedent conditions trigger floods in India (Nanditha & Mishra, 2022). We find that the
277 Ghaghara sub-basin of the Ganga river experienced the worst flood in September 1915, affecting more than 10,000
278 km² area of the sub-basin. A multi-day rainfall in late August and early September (1915) caused the worst flood
279 in the basin. The Kosi sub-basin of the Ganga river experienced the worst flood in August 1914, which affected
280 more than 5000 km² of the basin (Figure 5). Similarly, Bhagirathi and other sub-basins in the Ganga river basin
281 were affected by the worst flood in late September 1924, which inundated more than 12000 km² of the sub-basin.
282 Similarly, Gandak and Gomti river basins experienced the worst floods in 1948 and 1915, respectively. Our results
283 agree with the information presented in previous studies (Agarwal & Narain, 1991; Fredrick, 2017; Joshi, 2014;
284 D. K. Mishra, 2015; A. Singh et al., 2021). We find that most of the sub-basins of the Ganga river basin are prone
285 to large extents of flood inundation. Moreover, the worst floods in most sub-basins were caused by multi-day
286 precipitation, a prominent driver of floods in the Indian sub-continental river basins (Figure 5).

- Formatted: Font: Times New Roman
- Formatted: Font: Times New Roman, 10 pt
- Formatted: Font: Times New Roman
- Formatted: Font: Times New Roman
- Formatted: Font: Times New Roman
- Formatted: Font: Times New Roman
- Formatted: Font: Times New Roman
- Formatted: Font: Times New Roman
- Formatted: Font: Times New Roman, 10 pt
- Formatted: Font: Times New Roman
- Formatted: Font: Times New Roman
- Formatted: Font: Times New Roman, 10 pt
- Formatted: Font: Times New Roman
- Formatted: Font: Times New Roman

Formatted: Font: Times New Roman
 Formatted: Font: Times New Roman

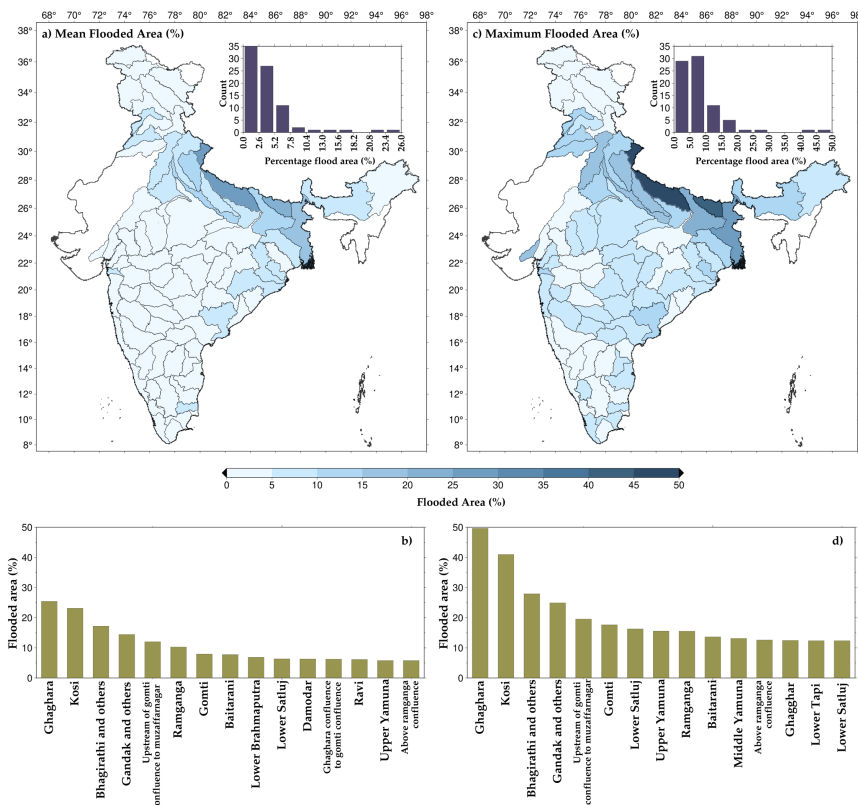


287

288 **Figure 5: Daily upstream precipitation (mm, blue), the H08 model simulated streamflow (red) at the sub-**
 289 **basin outlet (m3/s), and flooded area (km2, green) for the summer monsoon (June-September) period of**
 290 **the corresponding worst flood year. (a) Ghaghara - Ganga River basin (b) Kosi - Ganga River basin (c)**
 291 **Bhagirathi and others - Ganga River basin (d) Gandak and others - Ganga River basin (e) Upstream of**
 292 **Gomti confluence to Muzaffarnagar - Ganga River basin (f) Gomti - Ganga River basin (g) Lower**
 293 **Sabarmati – Sabarmati River basin (h) Upper Yamuna – Ganga River basin (i) Ramganga – Ganga River**
 294 **basin (j) Baitarani – Brahmani River basin**

295 To further examine the flood-affected area at the sub-basin level, we estimated the mean annual maximum flooded
 296 area (Figure 6a) and historical maximum flooded area using the H08-CaMa flood models (Figure 6b). Most of the
 297 highly flooded sub-basins are in the Ganga River basin. While the mean annual maximum flooded area for the
 298 top flood-affected sub-basins ranged between 10 to 15%, their maximum flooded area varied between 30 to 40%.
 299 Other than sub-basins from the Ganga river basin, Baitarani, lower Tapi, lower Godavari, Brahmani, and lower
 300 Mahanadi also showed a considerable mean flooded area during the 1901-1920 period. In the case of the maximum
 301 flooded area, Gandak, Kosi, and Ghaghara confluence to Gomti confluence sub-basins exhibited more than 20%
 302 flooded area. Sub-basins from the other river basins, such as lower Tapi, lower Narmada, Baitarani, and lower

303 Satluj, are in the top fifteen sub-basins with the highest flooded area. The sub-basins in the Ganga and
 304 Brahmaputra rivers are the most flood-affected. Moreover, the Ganga and Brahmaputra rivers experience the
 305 highest floods among all the river basins (Mohanty et al., 2020; Mohapatra & Singh, 2003).



Formatted: Font: Times New Roman
 Formatted: Font: Times New Roman, 10 pt
 Formatted: Font: Times New Roman
 Formatted: Font: Times New Roman
 Formatted: Font: Times New Roman
 Formatted: Font: Times New Roman

306
 307 **Figure 6: (a) Mean of annual maximum flooded area (percentage) between 1901-2020 and the overall**
 308 **distribution (b) highlighting the top fifteen sub-basin. (c) Historical maximum flooded area (percentage)**
 309 **and the overall distribution (d) highlighting the top fifteen sub-basin.**

310 **3.3 Influence of reservoirs on flood extent**

311 We selected and considered 51 major reservoirs to examine their influence on flood risk based on the availability
 312 of the observed storage data. We estimated C-ratio for each sub-basin considering the river flow at the outlet to
 313 investigate the impact of reservoirs on streamflow. C-ratio can vary between zero to infinity, and higher values
 314 indicate the prominent effect of dams on river flow. We identified sub-basins with a greater influence on dams
 315 based on the C-ratio. We find that Beas, Brahmani, upper Satluj, Upper Godavari, Middle and Lower Krishna,
 316 and Vashishti are among the most influenced by the dams. Beas sub-basin has the highest C-ratio (4.16) among
 317 all the sub-basin in the Indian sub-continent (Figure 7a). Out of the 80 sub-basins, only eleven have C-ratio greater

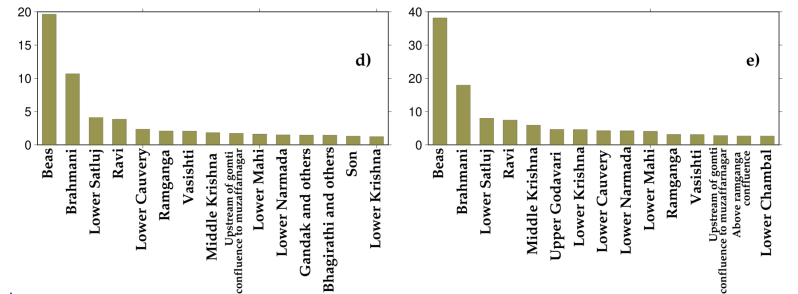
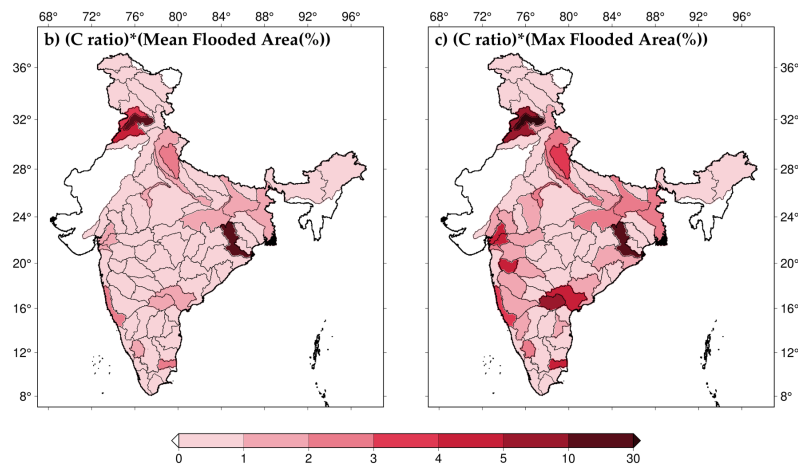
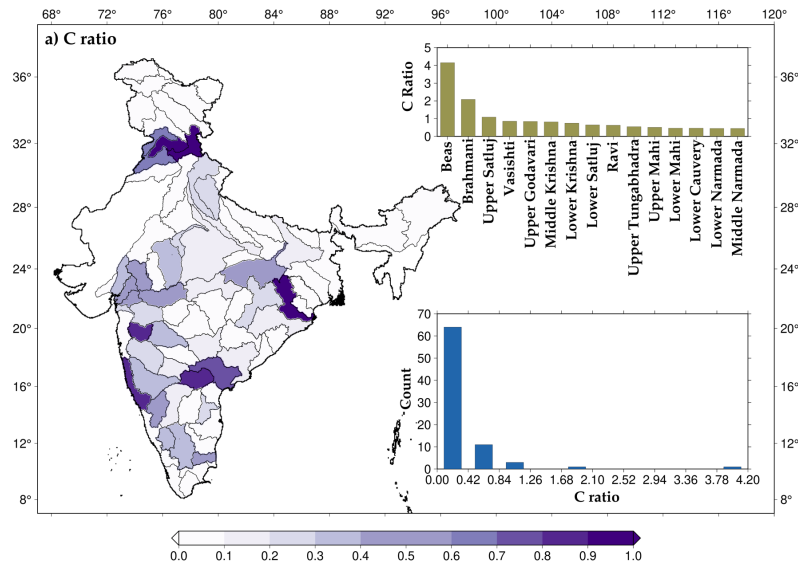
318 than 0.5. 64 out of 80 sub-basins have a C-ratio between zero to 0.42 (Figure 7a). We considered only 51 major
319 reservoirs in our analysis. However, there are several major and minor dams for which observed data is
320 unavailable. Therefore, the influence of reservoirs based on the C-ratio might need to be considered. However,
321 our analysis indicates that dams in a few sub-basins can significantly alter the river flow and flood risk. For
322 instance, dams effectively alter extreme flow's timing, duration, and frequency (Mittal et al., 2016). C-ratio alone
323 may not effectively capture the influence of dams on floods; therefore, we multiplied the fractional area affected
324 by floods and the C-ratio for each sub-basins. For instance, if a sub-basin is considerably affected by dams and
325 has a large flood extent, the value of the multiplied ratio will be higher. The multiplier ratio can effectively identify
326 the sub-basins with high flood-affected areas and flow regulated by the reservoirs. We find that Beas, Brahmani,
327 Ravi, and Lower Satluj are among the highly influenced by floods and the presence of reservoirs. Overall, the
328 sub-basins with higher C ratio and the highest flood-affected area are across the Indian subcontinent. Central India
329 has sub-basins that are relatively less affected by floods and the presence of dams.

Formatted: Font: Times New Roman

Formatted: Font: Times New Roman

Formatted: Font: Times New Roman

Formatted: Font: Times New Roman



Formatted: Font: Times New Roman

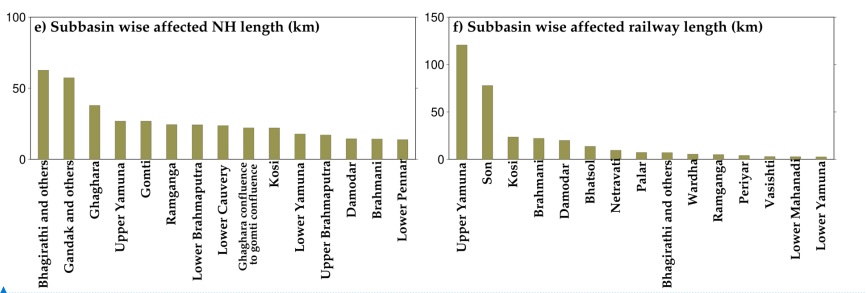
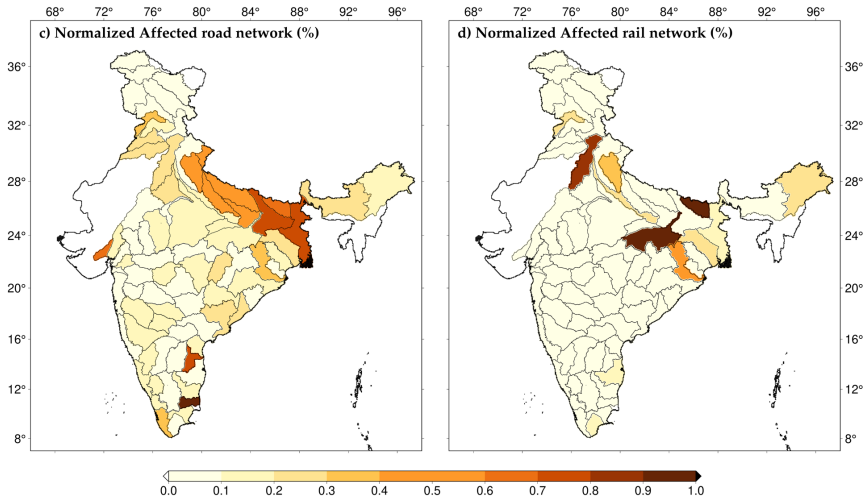
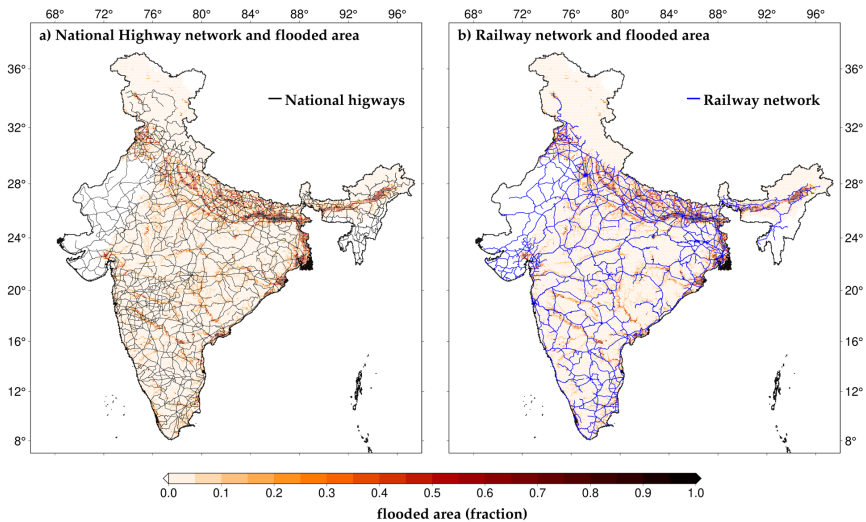
Formatted: Font: Times New Roman

331 **Figure 7: (a) Sub-basin wise C-ratio, top fifteen sub-basins and distribution of sub-basins based on C-ratio**
332 **values (b) Mean of annual maximum flooded area (percentage) multiplied with C-ratio (d) highlighting top**
333 **15 sub-basins (c) Historical maximum flooded area (percentage) multiplied with C-ratio (e) highlighting**
334 **top 15 sub-basins.**

335 3.4 Sub-basin level flood risk assessment

336 Next, we identified the roads (national highways) and railway exposure to riverine floods for each subbasin.
337 Climate change will adversely affect rail and road networks (Hooper & Chapman, 2012; Padhra, 2022). A
338 considerable length of roads is affected due to surface flooding resulting from high-intensity rain (Koks et al.,
339 2019). Therefore, we examined the impact of floods on rail and road infrastructure in India. We estimated the
340 length of the road and railway network potentially affected by the worst flood that occurred during 1901-2020.
341 We overlapped the road and rail network over the flooded area and estimated the network length exposed to floods
342 (Figures 8a-b). The estimated length for each sub-basin was normalized between zero and one (Figures 8c-d). We
343 find that the road network can be the most affected by the floods in the Gandak, Kosi and Ghaghara confluence
344 to Gomti confluence in the Ganga river basin. On the other hand, a considerable part of the rail network can be
345 affected by floods in Son, Kosi, and Upper Yamuna subbasins. Moreover, in Bhagirathi and Gandak river basins,
346 more than 50 km of road network falls in the flood-prone regions (Figure 8e). There are ten sub-basins in which
347 more than 20 km of road network falls in flood-prone areas of India. Similarly, over 20 km of the rail network is
348 in the flood-affected areas of the six sub-basins (Upper Yamuna, Son, Kosi, Brahmani) [Figure 8f].

- Formatted: Font: Times New Roman
- Formatted: Font: Times New Roman, 10 pt
- Formatted: Font: Times New Roman
- Formatted: Font: Times New Roman
- Formatted: Font: Times New Roman
- Formatted: Font: Times New Roman
- Formatted: Font: Times New Roman
- Formatted: Font: Times New Roman



Formatted: Font: Times New Roman

Formatted: Font: Times New Roman

350 **Figure 8: Flood impacts on roads and railways infrastructure. (a-b) National Highways network and**
351 **Railway network overlapped over the flooded area in worst flood cases, (c-d) subbasin wise normalised**
352 **flood affected road and railway network (percentage), (e-f) top 15 subbasins with most affected national**
353 **highways and railway length (km).**

354 Finally, we estimated sub-basin level flood risk using normalized vulnerability, hazard, and exposure (Figure 9).
355 Vulnerability for each sub-basin in India was assessed using the national vulnerability assessment data available
356 at the district level. We estimated hazard probability considering 50% of the inundated area for the worst flood as
357 a benchmark. The likelihood of flood inundated areas in a sub-basin exceeding the benchmark was used in the
358 risk assessment. Similarly, we used the worst flood extent and gridded population data to estimate flood exposure.
359 The sub-basins in north-central India have a relatively higher vulnerability calculated using the socio-economic
360 indicators. The vulnerability is relatively lower in north India and the Western Ghats. Kosi, Gandak, and Damodar
361 sub-basins have the highest vulnerability. We find that hazard probability is higher in the sub-basins of
362 Brahmaputra, rivers in the western Ghats, and a few sub-basins of the Indus river basin (Figure 9b). For instance,
363 upper Satluj, Chenab, and Jhelum sub-basins of the Indus river have higher hazard probability. Other than the
364 Western Ghats, most sub-basins in Peninsular India have relatively lesser hazard probability. Exposure, which
365 represents the fraction of the population affected by flood under the worst flood scenario, is higher in the Indo-
366 Gangetic Plain. Apart from the sub-basins of the Ganga River basin, the lower Brahmaputra, lower Godavari, and
367 Baitarani sub-basin show higher exposure. Therefore, Ganga and Brahmaputra Rivers basins are the highest flood-
368 prone river basins and have high flood exposure. [Rentschler et al. \(2022\)](#) also reported that the highest population
369 exposure due to floods is in Uttar Pradesh, Bihar, and West Bengal, which is part of the Ganga river basin.

Formatted: Font: Times New Roman

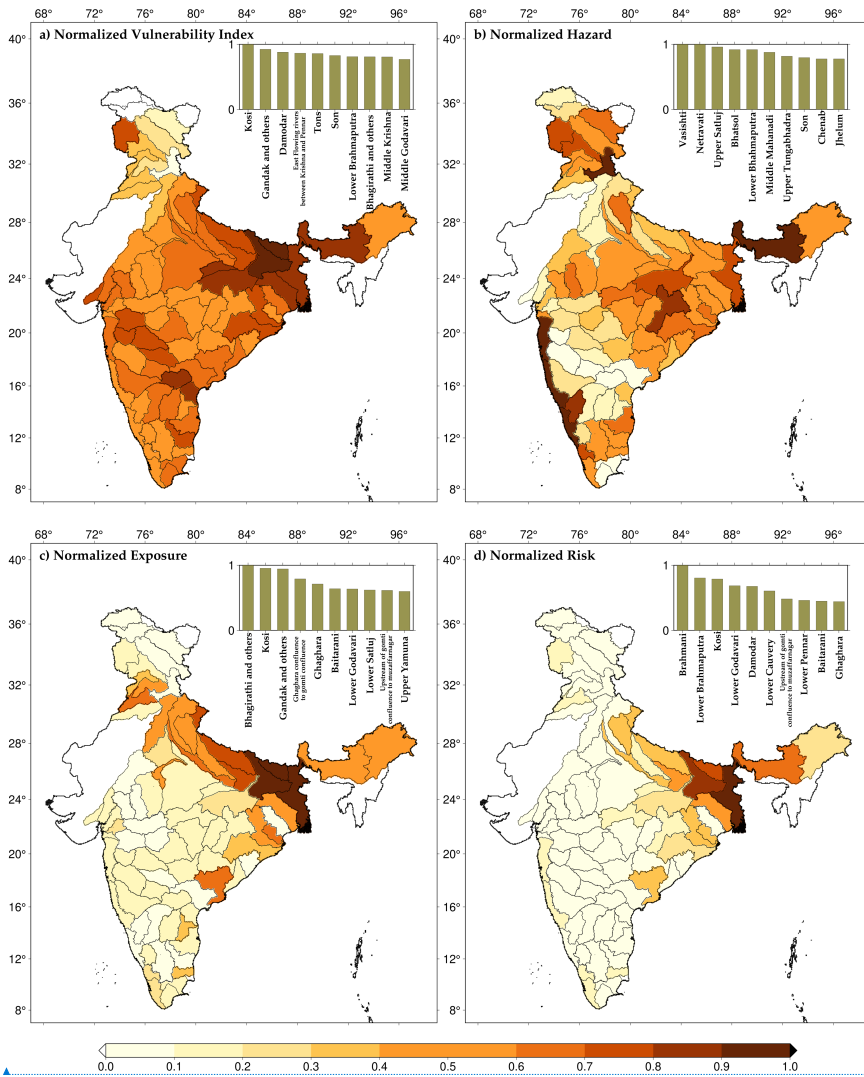
Formatted: Font: Times New Roman

Formatted: Font: Times New Roman

Formatted: Font: Times New Roman

Formatted: Font: Times New Roman

Formatted: Font: Times New Roman



370

371 **Figure 9: Sub-basin level (a) Normalized vulnerability index (b) Normalized hazard (c) Normalized**
372 **exposure (d) Normalized risk. The top 10 sub-basins are highlighted as bars in panels inside the figures.**

373 We estimated the flood risk for each sub-basin, a collective representation of vulnerability, hazard, and exposure.
374 As expected, the flood risk is higher in the Ganga and Brahmaputra river basins compared to other parts of the
375 country. The higher flood risk in these basins can be attributed to higher vulnerability, hazard probability, and
376 exposure. For instance, Bhagirathi, Gandak, Kosi, lower Brahmaputra, and Ghaghra are the sub-basins with the
377 highest flood risk in India (Figure 9d). Despite the higher hazard probability in the sub-basins of the Indus and

378 west coast river basins, the overall flood-risk is considerably lower than the sub-basins of the Ganga and
379 Brahmaputra river basins primarily due to less vulnerability and exposure. Our results show that flood risk in
380 some of the sub-basins of the Ganga and Brahmaputra river basins can be reduced by reducing the vulnerability.

381 4. Discussion and conclusions

382 Flood risk mapping is essential for risk reduction and developing mitigation measures. The flood risk will likely
383 increase due to increased hazard probability and exposure (Ali et al., 2019). Hirabayashi et al. (2013) showed that
384 a warmer climate would increase the risk of floods on a global scale. In India also, floods are expected to become
385 more likely under warming climate. For instance, Ali et al. (2019) reported that multi-day floods are projected to
386 rise faster than single-day flood events. The projected rise in the flood frequency in India can be attributed to
387 increased extreme precipitation under warming climate (Mukherjee et al., 2018). Observational studies have also
388 concluded that there has been a considerable rise in extreme precipitation in India during the summer monsoon
389 season (Roxy et al., 2017), which is linked to warming climate. While the warming climate is directly linked to
390 the increased frequency of extreme precipitation, its association with riverine floods is not straightforward. For
391 instance, Nanditha & Mishra (2021, 2022) reported that multi-day precipitation on the wet antecedent condition
392 is the most favourable conditions for riverine floods in India.

393 While mapping the flood risk at appropriate spatial resolution is complex and challenging, it is vital for disaster
394 risk reduction. Flood inundation mapping that provides the spatial extent of flooding is crucial as the first
395 responders use it during a flood emergency (Apel et al., 2009). There are several approaches to mapping flood
396 inundation (Teng et al., 2017). Various hydrological models have been employed for conducting flood risk
397 assessments at a global scale (Dottori et al., 2018; Gu et al., 2020; Tabari et al., 2021). For instance, Dottori et al.
398 (2018) used the H08 model combined with CaMa-Flood model to estimate losses resulting from river flooding at
399 the country level. Additionally, the LISFLOOD model (van der Knijff et al., 2010) at 5 km spatial resolution was
400 used to estimate the river flood risk in Europe (Alfieri et al., 2018). Flood risk assessment at relatively larger
401 scales are conducted using the coarse resolution land surface hydrological models. The objective of these large
402 scale flood risk assessment is to identify regions that are flood-prone (Dottori et al., 2018; Gu et al., 2020; Tabari
403 et al., 2021). On the other hand, high resolution flood inundation mapping is needed to understand the local flood
404 risk and damage caused to infrastructure. For the analysis of flood inundation during a particular flood at a local
405 scale, high-resolution models such as HEC-RAS and Mike FLOOD can be employed (Khalaj et al., 2021; Nguyen
406 et al., 2016). High resolution flood risk mapping requires comprehensive information of high-resolution
407 topography, cross-sections of channels, and data associated to structural measures of flood protection. However,
408 the smallest subbasin considered in our study has more than 5000 km² area (Fig S7), while most subbasins have
409 area between 10,000 and 50,000 km², with Lower Yamuna being the largest subbasin, with an area of 124,867.19
410 km². Therefore, the performance of our modelling framework against the satellite and other observations can be
411 considered satisfactory to provide a sub-basin scale flood risk assessment. Moreover, we used hydrodynamic
412 modelling to develop long-term flood inundation maps for the Indian sub-basins. The long-term data (1901-2020)
413 provides us a record of several floods, which can help in robust estimates of flood risk in different sub-basins.

414

Formatted: Font: Times New Roman

Formatted: Font: Times New Roman

Formatted: Font: Times New Roman

Formatted: Font: Times New Roman

Formatted: Font: Times New Roman

Formatted: Font: Times New Roman

Formatted: Font: Times New Roman

Formatted: Font: Times New Roman

Formatted: Font: Times New Roman

Formatted: Font: Times New Roman

Formatted: Font: Times New Roman

Formatted: Font: Times New Roman

Formatted: Font: Times New Roman

Formatted: Font: Times New Roman

Formatted: Font: Times New Roman

Formatted: Font: Times New Roman

Formatted: Font: Times New Roman

Formatted: Font: Times New Roman

Formatted: Font: Times New Roman

Formatted: Font: Times New Roman

Formatted: Font: Times New Roman

Formatted: Font: Times New Roman, 10 pt

Formatted: Font: Times New Roman

Formatted: Font: Times New Roman

Formatted: Font: Times New Roman

Formatted: Font: Times New Roman

Formatted: Font: Times New Roman

Formatted: Font: Times New Roman

Formatted: Font: Times New Roman

Deleted: We used hydrodynamic modelling to develop long-term flood inundation maps for the Indian sub-basins.

Formatted: Font: Times New Roman

Formatted: Font: Times New Roman

Formatted: Font: Times New Roman

417 While high-resolution models are suitable for event-specific finer-level flood assessments, their feasibility
418 diminishes in studies involving large-scale flood inundation over longer durations (Yamazaki et al., 2018b),
419 Creating high-resolution flood inundation maps based on hydrodynamic modelling is computationally expensive
420 (Dottori et al., 2016) for a large domain like India. In addition, higher-resolution flood risk mapping that can be
421 used at the local scale for decision-making requires accurate terrain information and river cross-section datasets
422 that are not available. For instance, freely available digital elevation models (DEM) can be too coarse to resolve
423 the flood inundation and depth variability at a local scale (Cook & Merwade, 2009; Dey et al., 2022). The
424 uncertainties within hydrologic outputs can primarily arise due to inaccuracies in both input data and model
425 parameterization (Poulin et al., 2011). Inaccuracies in input meteorological data may stem from disparate sources,
426 leading to errors in spatial and temporal interpolation (Brown & Heuvelink, 2005). Similarly, model
427 parameterization errors, which involve assigning values to parameters governing diverse hydrological processes,
428 can emerge during the calibration process (Laiolo et al., 2015). Moreover, there are uncertainties originating from
429 utilizing long-term flood occurrence data to assess flood mapping capabilities. Our modelling framework that
430 considers the influence of reservoirs provides sub-basin scale flood inundation extent as our aim was to provide a
431 long-term assessment of flood extent in at the country scale. Additionally, downscaling of flood depths introduces
432 biases as coarse-scale information is translated to the local scale (He et al., 2021), which might have considerable
433 deviations from the actual observed flood extent. Given these limitations, our findings provide valuable
434 information based on the long-term record developed using model simulations that can be used for the regional
435 scale policy development for flood mitigation. Cloud cover during the summer monsoon, when most floods occur
436 in India (Nanditha et al., 2022), hinders the utility of satellite data for flood inundation mapping. We calibrated
437 and evaluated our H08-CaMa flood modelling framework using the observed flow, reservoir storage, and satellite-
438 based inundation. However, all these datasets available from the in-situ network or satellites are prone to errors
439 and uncertainty (Di Baldassarre & Montanari, 2009; Stephens et al., 2012; Teng et al., 2017). We used C-ratio as
440 an indicator to quantify the influence of dams on streamflow. However, C-ratio may not fully capture the
441 complexities and variations in the impacts of reservoir operations. Furthermore, in case of run-of-the-river (RoR)
442 dams, the C-ratio may over-estimate the downstream hydrological impacts. Therefore, C-ratio may not solely
443 capture the downstream hydrological effects resulting from dams. Nevertheless, it provides preliminary
444 information on the potential dam influence on the downstream flow.

445 India has implemented several flood risk mitigation measures at multiple government levels. The construction of
446 embankments along rivers is a common flood risk mitigation measure in India. These embankments help contain
447 the floodwaters within the river channels and protect nearby areas from inundation (NDMA, 2016). The CWC in
448 India operates a network of flood forecasting stations that collect real-time data on rainfall and water levels to
449 forecast floods and issue warnings to vulnerable communities. Notwithstanding the considerable investments and
450 flood-control measures, India has witnessed substantial mortality, human migration, and economic loss. Flood
451 mortality has increased mainly because of increased frequency, not necessarily due to increased flood intensity
452 (Hu et al., 2018). About 3% of the total geographical area of India is affected by floods every year that cause
453 damage to agriculture and infrastructure. The top ten floods that occurred during 1985-2015 caused the mortality
454 of more than 1000 people while more than 35 million people were displaced due to floods between 2000-2004
455 (Dartmouth Flood Observatory). The recent riverine floods in Uttarakhand and Kerala highlighted the growing
456 flood risk in India, which warrants the need for flood mitigation. The recent flood in August 2022 in Pakistan

Formatted: Font: Times New Roman, Font colour: Black

Formatted: Font: Times New Roman

Formatted: Font: Times New Roman

Formatted: Font: Times New Roman

Formatted: Font: Times New Roman

Formatted: Font: Times New Roman

Formatted: Font: Times New Roman

Formatted: Font: Times New Roman, 10 pt

Formatted: Font: Times New Roman

Formatted: Font: Times New Roman

Formatted: Font: Times New Roman

Formatted: Font: Times New Roman

Formatted: Font: Times New Roman

Formatted: Font: Times New Roman

Formatted: Font: Times New Roman

Formatted: Font: Times New Roman, 10 pt

Formatted: Font: Times New Roman

Formatted: Font: Times New Roman

Formatted: Font: Times New Roman

Formatted: Font: Times New Roman

Formatted: Font: Times New Roman

Formatted: Font: Times New Roman

Formatted: Font: Times New Roman

Formatted: Font: Times New Roman

Formatted: Font: Times New Roman

Formatted: Font: Times New Roman

Formatted: Font: Times New Roman

Formatted: Font: Times New Roman

Formatted: Font: Times New Roman

Formatted: Font: Times New Roman

Formatted: Font: Times New Roman

Formatted: Font: Times New Roman, 10 pt

Formatted: Font: Times New Roman

Formatted: Font: Times New Roman

Formatted: Font: Times New Roman

Formatted: Font: Times New Roman

Formatted: Font: Times New Roman

Formatted: Font: Times New Roman

457 caused an estimated loss of \$30 billion. Both structural and non-structural measures are required for flood
458 mitigation (Nanditha & Mishra, 2021). Our risk assessment provides policy implications towards reducing
459 vulnerability to reduce the flood risk. Moreover, a sub-basin level ensemble forecast is needed to be used for early
460 flood warnings in the sub-basins with higher flood risk.

461 Based on our findings, the following conclusions can be made:

- 462 • The coupled hydrological and hydrodynamic modelling framework based on the H08-CaMa Flood model
463 was used to estimate the flood risk assessment in India. The hydrological modelling framework
464 performed well against the observed flow, reservoir storage, and satellite-based flood inundation. The
465 role of 51 major reservoirs was considered in flood risk assessment based on the long-term simulations
466 for the 1901-2020 period.
- 467 • The sub-basins in the Ganga and Brahmaputra river basins experienced the most significant flood extent
468 during the worst flood in 1901-2020. Similarly, the mean annual maximum flood extent is higher for the
469 sub-basins in the two major transboundary river basins (e.g., Ganga and Brahmaputra). The worst flood
470 affected different sub-basins on the two main flood-affected river basins in different years. Major floods
471 in the flood-prone sub-basins of the Ganga and Brahmaputra basins occur during the summer monsoon
472 season, especially during the August-September period.
- 473 • The sub-basins with a more prominent influence of dams based on the C-ratio were identified. Beas,
474 Brahmani, upper Satluj, Upper Godavari, Middle and Lower Krishna, and Vashishti sub-basins are
475 among the most influenced by the dams. Moreover, Beas, Brahmani, Ravi, and Lower Satluj are among
476 the most affected by floods and the presence of reservoirs.
- 477 • Flood risk is higher in the Ganga and Brahmaputra river basins compared to other parts of the country.
478 The higher flood risk in the two transboundary river basins can be attributed to higher vulnerability,
479 hazard probability, and exposure. Bhagirathi, Gandak, Kosi, lower Brahmaputra, and Ghaghra are India's
480 sub-basins with the highest flood risk.

Formatted: Font: Times New Roman

Formatted: Font: Times New Roman, 10 pt

Formatted: Font: Times New Roman

Formatted: Font: Times New Roman

481 **Data availability:** All the datasets used in this study can be obtained from the corresponding author.

482 **Competing interest:** Authors declare no competing interest.

483 **Author contributions:** VM designed the study. UV conducted the analysis and wrote the first draft. All the
484 authors contributed in the writing and discussion.

485 **Acknowledgement:** The work was supported by the Monsoon Mission, Ministry of Earth Sciences. The
486 authors acknowledge the data availability from India Meteorological Department (IMD) and India-WRIS.
487 We acknowledge the database availability from EM-DAT: <http://www.emdat.be/>, DFO:
488 <http://floodobservatory.colorado.edu>, population data from GHSL:
489 <https://sedac.ciesin.columbia.edu/data/set/ghsl-population-built-up-estimates-degree-urban-smod>,
490 vulnerability assessment data from DST: HYPERLINK
491 "https://dst.gov.in/sites/default/files/Full%20Report%20%281%29.pdf" <https://dst.gov.in/sites/default/files/Full%20Report%20%281%29.pdf>
492 <https://dst.gov.in/sites/default/files/Full%20Report%20%281%29.pdf>.

493 References

- 494 Acreman, M. (2000). *Managed Flood Releases from Reservoirs: Issues and*
495 *Guidance*.
496 [https://sswm.info/sites/default/files/reference_attachments/ACREMAN%202000](https://sswm.info/sites/default/files/reference_attachments/ACREMAN%202000%20Managed%20Flood%20Releases%20from%20Reservoirs.pdf)
497 [0%20Managed%20Flood%20Releases%20from%20Reservoirs.pdf](https://sswm.info/sites/default/files/reference_attachments/ACREMAN%202000%20Managed%20Flood%20Releases%20from%20Reservoirs.pdf)
- 498 Agarwal, A., & Narain, S. (1991). *Floods, flood plains and environmental myths*.
- 499 [Alfieri, L., Dottori, F., Betts, R., Salamon, P., & Feyen, L. \(2018\). Multi-Model Projections of](https://doi.org/10.3390/CLI6010006)
500 [River Flood Risk in Europe under Global Warming. *Climate 2018, Vol. 6, Page 6, 6\(1\), 6.*](https://doi.org/10.3390/CLI6010006)
501 <https://doi.org/10.3390/CLI6010006>
- 502 Ali, H., Modi, P., & Mishra, V. (2019). Increased flood risk in Indian sub-continent
503 under the warming climate. *Weather and Climate Extremes*, 25, 100212.
504 <https://doi.org/10.1016/J.WACE.2019.100212>
- 505 Allen, S. K., Linsbauer, A., Randhawa, S. S., Huggel, C., Rana, P., & Kumari, A.
506 (2016). Glacial lake outburst flood risk in Himachal Pradesh, India: an
507 integrative and anticipatory approach considering current and future threats.
508 *Natural Hazards*, 84(3), 1741–1763. <https://doi.org/10.1007/s11069-016-2511-x>
- 509 Apel, H., Aronica, G. T., Kreibich, H., & Thielen, A. H. (2009). Flood risk analyses -
510 How detailed do we need to be? *Natural Hazards*, 49(1), 79–98.
511 <https://doi.org/10.1007/S11069-008-9277-8/TABLES/5>
- 512 Bernhofen, M. V., Cooper, S., Trigg, M., Mdee, A., Carr, A., Bhave, A., Solano-
513 Correa, Y. T., Pencue-Fierro, E. L., Teferi, E., Haile, A. T., Yusop, Z., Alias, N.
514 E., Sa'adi, Z., Bin Ramzan, M. A., Dhanya, C. T., & Shukla, P. (2022). The
515 Role of Global Data Sets for Riverine Flood Risk Management at National
516 Scales. *Water Resources Research*, 58(4).
517 <https://doi.org/10.1029/2021wr031555>

Formatted: Line spacing: 1.5 lines

Formatted: Indent: Left: 0.85 cm, First line: 0 cm, Line spacing: 1.5 lines, Adjust space between Latin and Asian text, Adjust space between Asian text and numbers

Formatted: No underline, Font colour: Auto,

- 518 Birkmann, J., & Welle, T. (2015). Assessing the risk of loss and damage: Exposure,
519 vulnerability and risk to climate-related hazards for different country
520 classifications. *International Journal of Global Warming*, 8(2), 191–212.
521 <https://doi.org/10.1504/IJGW.2015.071963>
- 522 Boulange, J., Hanasaki, N., Yamazaki, D., & Pokhrel, Y. (2021). Role of dams in
523 reducing global flood exposure under climate change. *Nature Communications*,
524 12(1). <https://doi.org/10.1038/s41467-020-20704-0>
- 525 Brown, J. D., & Heuvelink, G. B. M. (2005). Assessing Uncertainty Propagation
526 through Physically Based Models of Soil Water Flow and Solute Transport.
527 *Encyclopedia of Hydrological Sciences*.
528 <https://doi.org/10.1002/0470848944.HSA081>
- 529 Chaudhari, S., & Pokhrel, Y. (2022). Alteration of River Flow and Flood Dynamics
530 by Existing and Planned Hydropower Dams in the Amazon River Basin. *Water*
531 *Resources Research*, 58(5). <https://doi.org/10.1029/2021WR030555>
- 532 [Chuphal, D. S., & Mishra, V. \(2023\). Hydrological model-based streamflow reconstruction for](https://doi.org/10.1038/s41597-023-02618-w)
533 [Indian sub-continental river basins, 1951–2021. *Scientific Data* 2023 10:1, 10\(1\), 1–11.](https://doi.org/10.1038/s41597-023-02618-w)
534 <https://doi.org/10.1038/s41597-023-02618-w>
- 535 Cook, A., & Merwade, V. (2009). Effect of topographic data, geometric configuration
536 and modeling approach on flood inundation mapping. *Journal of Hydrology*,
537 377(1–2), 131–142. <https://doi.org/10.1016/J.JHYDROL.2009.08.015>
- 538 Dang, H., Pokhrel, Y., Shin, S., Stelly, J., Ahlquist, D., & Du Bui, D. (2022).
539 Hydrologic balance and inundation dynamics of Southeast Asia’s largest inland
540 lake altered by hydropower dams in the Mekong River basin. *Science of The*
541 *Total Environment*, 831, 154833.
542 <https://doi.org/10.1016/J.SCITOTENV.2022.154833>
- 543 Dang, T. D., Chowdhury, A. K., & Galelli, S. (2019). On the representation of water
544 reservoir storage and operations in large-scale hydrological models:
545 implications on model parameterization and climate change impact assessments.
546 *Hydrology and Earth System Sciences Discussions*, 1–34.
547 <https://doi.org/10.5194/hess-2019-334>
- 548 [Dangar, S., & Mishra, V. \(2021\). Natural and anthropogenic drivers of the lost groundwater](https://doi.org/10.1088/1748-9326/ac2ceb)
549 [from the Ganga River basin. *Environmental Research Letters*, 16\(11\).](https://doi.org/10.1088/1748-9326/ac2ceb)
550 <https://doi.org/10.1088/1748-9326/ac2ceb>
- 551 de Moel, H., Jongman, B., Kreibich, H., Merz, B., Penning-Rowsell, E., & Ward, P.
552 J. (2015). Flood risk assessments at different spatial scales. *Mitigation and*
553 *Adaptation Strategies for Global Change*, 20(6), 865–890.
554 <https://doi.org/10.1007/s11027-015-9654-z>
- 555 Dey, S., Saksena, S., Winter, D., Merwade, V., & McMillan, S. (2022). Incorporating
556 Network Scale River Bathymetry to Improve Characterization of Fluvial
557 Processes in Flood Modeling. *Water Resources Research*, 58(11),
558 e2020WR029521. <https://doi.org/10.1029/2020WR029521>

- 559 Di Baldassarre, G., & Montanari, A. (2009). Uncertainty in river discharge
560 observations: A quantitative analysis. *Hydrology and Earth System Sciences*,
561 13(6), 913–921. <https://doi.org/10.5194/HESS-13-913-2009>
- 562 Dottori, F., Salamon, P., Bianchi, A., Alfieri, L., Hirpa, F. A., & Feyen, L. (2016).
563 Development and evaluation of a framework for global flood hazard mapping.
564 *Advances in Water Resources*, 94, 87–102.
565 <https://doi.org/10.1016/J.ADVWATRES.2016.05.002>
- 566 [Dottori, F., Szewczyk, W., Ciscar, J. C., Zhao, F., Alfieri, L., Hirabayashi, Y., Bianchi, A.,
567 Mongelli, I., Frieler, K., Betts, R. A., & Feyen, L. \(2018\). Increased human and economic
568 losses from river flooding with anthropogenic warming. *Nature Climate Change* 2018 8:9,
569 8\(9\), 781–786. <https://doi.org/10.1038/s41558-018-0257-z>](#)
- 570 [Duc Dang, T., Kamal Chowdhury, A. F. M., & Galelli, S. \(2020\). On the representation of water
571 reservoir storage and operations in large-scale hydrological models: Implications on model
572 parameterization and climate change impact assessments. *Hydrology and Earth System
573 Sciences*, 24\(1\), 397–416. <https://doi.org/10.5194/HESS-24-397-2020>](#)
- 574 Eidsvig, U. M. K., Kristensen, K., & Vangelsten, B. V. (2017). Assessing the risk
575 posed by natural hazards to infrastructures. *Natural Hazards and Earth System
576 Sciences*, 17(3), 481–504. <https://doi.org/10.5194/nhess-17-481-2017>
- 577 Fredrick, O. (2017, May 19). Excavators allege debris was used to bury storey in
578 Chhatar Manzil. *Hindustan Times*.
579 [https://www.hindustantimes.com/lucknow/excavators-allege-debris-was-used-
580 to-bury-storey-in-chhatar-manzil/story-mMm8Dwog3azR6SSEmpvJIO.html](https://www.hindustantimes.com/lucknow/excavators-allege-debris-was-used-to-bury-storey-in-chhatar-manzil/story-mMm8Dwog3azR6SSEmpvJIO.html)
- 581 Gaur, A., & Gaur, A. (2018). *Future Changes in Flood Hazards across Canada
582 under a Changing Climate*. <https://doi.org/10.3390/w10101441>
- 583 Ghosh, A., & Kar, S. K. (2018). Application of analytical hierarchy process (AHP)
584 for flood risk assessment: a case study in Malda district of West Bengal, India.
585 *Natural Hazards*, 94(1), 349–368. <https://doi.org/10.1007/s11069-018-3392-y>
- 586 [Gu, X., Zhang, Q., Li, J., Chen, D., Singh, V. P., Zhang, Y., Liu, J., Shen, Z., & Yu, H. \(2020\).
587 Impacts of anthropogenic warming and uneven regional socio-economic development on
588 global river flood risk. <https://doi.org/10.1016/j.jhydrol.2020.125262>](#)
- 589 Hanasaki, N., Kanae, S., Oki, T., Masuda, K., Motoya, K., Shirakawa, N., Shen, Y.,
590 & Tanaka, K. (2008). An integrated model for the assessment of global water
591 resources - Part I: Model description and input meteorological forcing.
592 *Hydrology and Earth System Sciences*, 12(4), 1007–1025.
593 <https://doi.org/10.5194/HESS-12-1007-2008>
- 594 Hanasaki, N., Yoshikawa, S., Pokhrel, Y., & Kanae, S. (2018). A global hydrological
595 simulation to specify the sources of water used by humans. *Hydrology and
596 Earth System Sciences*, 22(1), 789–817. [https://doi.org/10.5194/hess-22-789-
597 2018](https://doi.org/10.5194/hess-22-789-2018)

- 598 He, X., Bryant, B. P., Moran, T., Mach, K. J., Wei, Z., & Freyberg, D. L. (2021).
599 Climate-informed hydrologic modeling and policy typology to guide managed
600 aquifer recharge. *Science Advances*, 7(17), 6025–6046.
601 https://doi.org/10.1126/SCIADV.ABE6025/SUPPL_FILE/ABE6025_SM.PDF
- 602 Hirabayashi, Y., Mahendran, R., Koirala, S., Konoshima, L., Yamazaki, D.,
603 Watanabe, S., Kim, H., & Kanae, S. (2013). Global flood risk under climate
604 change. *Nature Climate Change*, 3(9), 816–821.
605 <https://doi.org/10.1038/nclimate1911>
- 606 Hirabayashi, Y., Tanoue, M., Sasaki, O., Zhou, X., & Yamazaki, D. (2021). Global
607 exposure to flooding from the new CMIP6 climate model projections. *Scientific*
608 *Reports*, 0123456789, 1–7. <https://doi.org/10.1038/s41598-021-83279-w>
- 609 Hochrainer-Stigler, S., Schinko, T., Hof, A., & Ward, P. J. (2021). Adaptive risk
610 management strategies for governments under future climate and socioeconomic
611 change: An application to riverine flood risk at the global level. *Environmental*
612 *Science and Policy*, 125, 10–20. <https://doi.org/10.1016/j.envsci.2021.08.010>
- 613 Hooper, E., & Chapman, L. (2012). The impacts of climate change on national road
614 and rail networks. In *Transport and Sustainability* (Vol. 2, pp. 105–136).
615 Emerald Group Publishing Ltd. [https://doi.org/10.1108/S2044-](https://doi.org/10.1108/S2044-9941(2012)0000002008)
616 [9941\(2012\)0000002008](https://doi.org/10.1108/S2044-9941(2012)0000002008)
- 617 Hu, P., Zhang, Q., Shi, P., Chen, B., & Fang, J. (2018). Flood-induced mortality
618 across the globe: Spatiotemporal pattern and influencing factors. *Science of The*
619 *Total Environment*, 643, 171–182.
620 <https://doi.org/10.1016/J.SCITOTENV.2018.06.197>
- 621 IPCC. (2014). *Climate Change 2014: Synthesis Report. Contribution of Working*
622 *Groups I, II, and III to the Fifth Assessment Report of the. Geneva, Switzerland:*
623 *Intergovernmental Panel on Climate Change.*
- 624 Jain, G., Singh, C., Coelho, K., & Malladi, T. (2017). *Long-term implications of*
625 *humanitarian responses The case of Chennai.*
626 <http://pubs.iied.org/10840IIEDwww.iied.org@iiedwww.facebook.com/theIIED>
- 627 Joint Research Centre (JRC), European Commission and Center for International
628 Earth Science Information Network (CIESIN), & Columbia University. (2021).
629 *Global Human Settlement Layer: Population and Built-Up Estimates, and*
630 *Degree of Urbanization Settlement Model Grid. Palisades, NY: NASA*
631 *Socioeconomic Data and Applications Center (SEDAC).*
632 <https://doi.org/10.7927/h4154f0w>
- 633 Joshi, V. (2014, September 14). Have we learnt from past floods? Clearly not!
634 *Hindustan Times (Lucknow).* [https://www.pressreader.com/india/hindustan-](https://www.pressreader.com/india/hindustan-times-lucknow/20140914/281646778342401)
635 [times-lucknow/20140914/281646778342401](https://www.pressreader.com/india/hindustan-times-lucknow/20140914/281646778342401)
- 636 Kalantari, Z., Briel, A., Lyon, S. W., Olofsson, B., & Folkesson, L. (2014). On the
637 utilization of hydrological modelling for road drainage design under climate and

- 638 land use change. *Science of the Total Environment*, 475, 97–103.
639 <https://doi.org/10.1016/J.SCITOTENV.2013.12.114>
- 640 [Khalaj, M. R., Noor, H., & Dastranj, A. \(2021\). Investigation and simulation of flood inundation](#)
641 [hazard in urban areas in Iran. *Geoenvironmental Disasters*, 8\(1\), 1–13.](#)
642 <https://doi.org/10.1186/S40677-021-00191-1/FIGURES/11>
- 643 Kimuli, J. B., Di, B., Zhang, R., Wu, S., Li, J., & Yin, W. (2021). A multisource trend
644 analysis of floods in Asia-Pacific 1990–2018: Implications for climate change in
645 sustainable development goals. In *International Journal of Disaster Risk*
646 *Reduction* (Vol. 59). Elsevier Ltd. <https://doi.org/10.1016/j.ijdr.2021.102237>
- 647 Koks, E. E., Rozenberg, J., Zorn, C., Tariverdi, M., Vousdoukas, M., Fraser, S. A.,
648 Hall, J. W., & Hallegatte, S. (2019). A global multi-hazard risk analysis of road
649 and railway infrastructure assets. *Nature Communications*, 10(1).
650 <https://doi.org/10.1038/s41467-019-10442-3>
- 651 [Krysanova, V., Donnelly, C., Gelfan, A., Gerten, D., Arheimer, B., Hattermann, F., &](#)
652 [Kundzewicz, Z. W. \(2018\). How the performance of hydrological models relates to](#)
653 [credibility of projections under climate change. *Hydrological Sciences Journal*, 63\(5\),](#)
654 [696–720. <https://doi.org/10.1080/02626667.2018.1446214>](#)
- 655 Kushwaha, A. P., Tiwari, A. D., Dangar, S., Shah, H., Mahto, S. S., & Mishra, V.
656 (2021). Multimodel assessment of water budget in Indian sub-continental river
657 basins. *Journal of Hydrology*, 603, 126977.
658 <https://doi.org/10.1016/J.JHYDROL.2021.126977>
- 659 Laiolo, P., Gabellani, S., Campo, L., Cenci, L., Silvestro, F., Delogu, F., Boni, G.,
660 Rudari, R., Puca, S., & Pisani, A. R. (2015). Assimilation of remote sensing
661 observations into a continuous distributed hydrological model: Impacts on the
662 hydrologic cycle. *International Geoscience and Remote Sensing Symposium*
663 *(IGARSS), 2015-November*, 1308–1311.
664 <https://doi.org/10.1109/IGARSS.2015.7326015>
- 665 Lehner, B., Liermann, C. R., Revenga, C., Vörösmarty, C., Fekete, B., Crouzet, P.,
666 Döll, P., Endejan, M., Frenken, K., Magome, J., Nilsson, C., Robertson, J. C.,
667 Rödel, R., Sindorf, N., & Wisser, D. (2011). High-resolution mapping of the
668 world's reservoirs and dams for sustainable river-flow management. In
669 *Frontiers in Ecology and the Environment* (Vol. 9, Issue 9, pp. 494–502).
670 <https://doi.org/10.1890/100125>
- 671 Marchand, M., Dahm, R., Buurman, J., Sethurathinam, S., & Sprengers, C. (2022).
672 Flood protection by embankments in the Brahmani–Baitarani river basin, India:
673 a risk-based approach. *International Journal of Water Resources Development*,
674 38(2), 242–261. <https://doi.org/10.1080/07900627.2021.1899899>
- 675 Mateo, C. M., Hanasaki, N., Komori, D., & Tanaka, K. (2014). Assessing the impacts
676 of reservoir operation to floodplain inundation by combining hydrological,
677 reservoir management, and hydrodynamic models. *AGU Publications*, 7245–
678 7266. <https://doi.org/10.1002/2013WR014845>.Received

- 679 Mateo, C. M. R., Hanasaki, N., Komori, D., Yoshimura, K., Kiguchi, M.,
680 Champathong, A., Yamazaki, D., Sukhapunphan, T., & Oki, T. (2013). A
681 simulation study on modifying reservoir operation rules: Tradeoffs between
682 flood mitigation and water supply. *IAHS-AISH Proceedings and Reports*,
683 362(July), 33–40.
- 684 Mateo, C. M. R., Hanasaki, N., Komori, D., Yoshimura, K., Kiguchi, M.,
685 Champathong, A., Yamazaki, D., Sukhapunphan, T., & Oki, T. (2014). Flood
686 risk and climate change: global and regional perspectives. *Hydrological
687 Sciences Journal*, 59(1), 1–28. <https://doi.org/10.1080/02626667.2013.857411>
- 688 Mishra, D. K. (2015, March 10). 1948 Floods in Bihar-2 Inaugural flood after
689 Independence – Official Version of Floods and its Aftermath. *SANDRP*.
690 [https://sandrp.in/2015/03/10/1948-floods-in-bihar-2-inaugural-flood-after-
691 independence-official-version-of-floods-and-its-aftermath/](https://sandrp.in/2015/03/10/1948-floods-in-bihar-2-inaugural-flood-after-independence-official-version-of-floods-and-its-aftermath/)
- 692 Mishra, V., & Shah, H. L. (2018). Hydroclimatological Perspective of the Kerala
693 Flood of 2018. *Journal of the Geological Society of India*, 92(5), 645–650.
694 <https://doi.org/10.1007/s12594-018-1079-3>
- 695 Mishra, V., Tiwari, A. D., & Kumar, R. (2022). Warming climate and ENSO
696 variability enhance the risk of sequential extremes in India. *One Earth*, 5(11),
697 1250–1259. <https://doi.org/10.1016/J.ONEEAR.2022.10.013>
- 698 Mittal, N., Bhawe, A. G., Mishra, A., & Singh, R. (2016). Impact of human
699 intervention and climate change on natural flow regime. *Water Resources
700 Management*, 30(2), 685–699. <https://doi.org/10.1007/s11269-015-1185-6>
- 701 Mohanty, M. P., Mudgil, S., & Karmakar, S. (2020). Flood management in India: A
702 focussed review on the current status and future challenges. In *International
703 Journal of Disaster Risk Reduction* (Vol. 49). Elsevier Ltd.
704 <https://doi.org/10.1016/j.ijdr.2020.101660>
- 705 Mohapatra, P. K., & Singh, R. D. (2003). Flood management in India. *Natural
706 Hazards*, 28, 131–143. <https://doi.org/10.1177/0019556120120109>
- 707 Mukherjee, S., Aadhar, S., Stone, D., & Mishra, V. (2018). Increase in extreme
708 precipitation events under anthropogenic warming in India. *Weather and
709 Climate Extremes*, 20, 45–53. <https://doi.org/10.1016/J.WACE.2018.03.005>
- 710 Nanditha, J. S., Kushwaha, A. P., Singh, R., Malik, I., Solanki, H., Singh Chupal, D.,
711 Dangar, S., Shwarup Mahto, S., Mishra, V., Vegad, U., Chuphal, D. S., &
712 Mahto, S. S. (2022). The Pakistan flood of August 2022: causes and
713 implications. *Authorea Preprints*. <https://doi.org/10.1002/ESSOAR.10512560.1>
- 714 Nanditha, J. S., & Mishra, V. (2021). On the need of ensemble flood forecast in India.
715 *Water Security*, 12, 100086. <https://doi.org/10.1016/J.WASEC.2021.100086>
- 716 Nanditha, J. S., & Mishra, V. (2022). Multiday Precipitation Is a Prominent Driver of
717 Floods in Indian River Basins. *Water Resources Research*, 58(7),
718 e2022WR032723. <https://doi.org/10.1029/2022WR032723>

- 719 [Nguyen, P., Thorstensen, A., Sorooshian, S., Hsu, K., AghaKouchak, A., Sanders, B., Koren, V.,](#)
720 [Cui, Z., & Smith, M. \(2016\). A high resolution coupled hydrologic-hydraulic model](#)
721 [\(HiResFlood-UCL\) for flash flood modeling. *Journal of Hydrology*, 541, 401–420.](#)
722 <https://doi.org/10.1016/J.JHYDROL.2015.10.047>
- 723 Nilsson, C., Catherine, *, Reidy, A., Dynesius, M., & Revenga, C. (2005).
724 Fragmentation and Flow Regulation of the World’s Large River Systems. In
725 *SCIENCE* (Vol. 308). www.sciencemag.org
- 726 Padhra, A. (2022). Tourism in India and the Impact of Weather and Climate. In
727 *Indian Tourism* (pp. 187–197). Emerald Publishing Limited.
728 <https://doi.org/10.1108/978-1-80262-937-820221013>
- 729 Pai, D. S., Sridhar, L., Rajeevan, M., Sreejith, O. P., Satbhai, N. S., &
730 Mukhopadhyay, B. (2014). Development of a new high spatial resolution (0.25°
731 × 0.25°) long period (1901-2010) daily gridded rainfall data set over India and
732 its comparison with existing data sets over the region. *Mausam*, 65(1), 1–18.
- 733 Pathak, S., Liu, M., Jato-Espino, D., & Zevenbergen, C. (2020). Social, economic and
734 environmental assessment of urban sub-catchment flood risks using a multi-
735 criteria approach: A case study in Mumbai City, India. *Journal of Hydrology*,
736 591, 125216. <https://doi.org/10.1016/J.JHYDROL.2020.125216>
- 737 Peduzzi, P., Dao, H., Herold, C., & Mouton, F. (2009). Natural Hazards and Earth
738 System Sciences Assessing global exposure and vulnerability towards natural
739 hazards: the Disaster Risk Index. In *Hazards Earth Syst. Sci* (Vol. 9). www.nat-
740 hazards-earth-syst-sci.net/9/1149/2009/
- 741 Pekel, J. F., Cottam, A., Gorelick, N., & Belward, A. S. (2016). High-resolution
742 mapping of global surface water and its long-term changes. *Nature*, 540(7633),
743 418–422. <https://doi.org/10.1038/nature20584>
- 744 Pokhrel, Y., Shin, S., Lin, Z., Yamazaki, D., & Qi, J. (2018). Potential Disruption of
745 Flood Dynamics in the Lower Mekong River Basin Due to Upstream Flow
746 Regulation. *Scientific Reports*, 8(1). [https://doi.org/10.1038/s41598-018-35823-](https://doi.org/10.1038/s41598-018-35823-4)
747 4
- 748 Poulin, A., Brissette, F., Leconte, R., Arsenault, R., & Malo, J. S. (2011). Uncertainty
749 of hydrological modelling in climate change impact studies in a Canadian,
750 snow-dominated river basin. *Journal of Hydrology*, 409(3–4), 626–636.
751 <https://doi.org/10.1016/J.JHYDROL.2011.08.057>
- 752 [Raghav, P., & Eldho, T. I. \(2023\). Investigations on the hydrological impacts of climate change](#)
753 [on a river basin using macroscale model H08. *Journal of Earth System Science*, 132\(2\), 1–](#)
754 [23. <https://doi.org/10.1007/S12040-023-02102-4/FIGURES/10>](#)
- 755 Rentschler, J., Salhab, M., & Jafino, B. A. (2022). Flood exposure and poverty in 188
756 countries. *Nature Communications*, 13(1). [https://doi.org/10.1038/s41467-022-](https://doi.org/10.1038/s41467-022-30727-4)
757 30727-4

758 Roxy, M. K., Ghosh, S., Pathak, A., Athulya, R., Mujumdar, M., Murtugudde, R.,
759 Terray, P., & Rajeevan, M. (2017). A threefold rise in widespread extreme rain
760 events over central India. *Nature Communications*, 8(1).
761 <https://doi.org/10.1038/s41467-017-00744-9>

762 Roy, B., Khan, M. S. M., Saiful Islam, A. K. M., Khan, M. J. U., & Mohammed, K.
763 (2021). Integrated flood risk assessment of the arial khan river under changing
764 climate using ipcc ar5 risk framework. *Journal of Water and Climate Change*,
765 12(7), 3421–3447. <https://doi.org/10.2166/wcc.2021.341>

766 Shah, H. L., & Mishra, V. (2016). Hydrologic Changes in Indian Subcontinental
767 River Basins (1901–2012). *Journal of Hydrometeorology*, 17(10), 2667–2687.
768 <https://doi.org/10.1175/JHM-D-15-0231.1>

769 Sheffield, J., Goteti, G., & Wood, E. F. (2006). *Development of a 50-Year High-*
770 *Resolution Global Dataset of Meteorological Forcings for Land Surface*
771 *Modeling*.

772 Singh, A., Mani, M., & Vishnoi, R. K. (2021). Tehri Dam–A Savior from Climate
773 Change Led Extreme Events. *INCOLD Journal (A Half Yearly Technical*
774 *Journal of Indian Committee on Large Dams)*, 10(2), 44–50.

775 Singh, P., Sinha, V. S. P., Vijhani, A., & Pahuja, N. (2018). Vulnerability assessment
776 of urban road network from urban flood. *International Journal of Disaster Risk*
777 *Reduction*, 28, 237–250. <https://doi.org/10.1016/J.IJDRR.2018.03.017>

778 Smith, A., Bates, P. D., Wing, O., Sampson, C., Quinn, N., & Neal, J. (2019). New
779 estimates of flood exposure in developing countries using high-resolution
780 population data. *Nature Communications*, 10(1).
781 <https://doi.org/10.1038/s41467-019-09282-y>

782 Srivastava, A. K., Rajeevan, M., & Kshirsagar, S. R. (2009). Development of a high
783 resolution daily gridded temperature data set (1969 – 2005) for the Indian
784 region. *Atmospheric Science Letters*, 10(October), 249–254.
785 <https://doi.org/10.1002/asl>

786 Stephens, E. M., Bates, P. D., Freer, J. E., & Mason, D. C. (2012). The impact of
787 uncertainty in satellite data on the assessment of flood inundation models.
788 *Journal of Hydrology*, 414–415, 162–173.
789 <https://doi.org/10.1016/J.JHYDROL.2011.10.040>

790 [Tabari, H., Hosseinzadehtalaei, P., Thiery, W., & Willems, P. \(2021\). Amplified Drought and](https://doi.org/10.1029/2021EF002295)
791 [Flood Risk Under Future Socioeconomic and Climatic Change. *Earth's Future*, 9\(10\),](https://doi.org/10.1029/2021EF002295)
792 [e2021EF002295. https://doi.org/10.1029/2021EF002295](https://doi.org/10.1029/2021EF002295)

793 Tanoue, M. (2020). *Future river-flood damage increases under aggressive*
794 *adaptations*. 1–12.

795 Teng, J., Jakeman, A. J., Vaze, J., Croke, B. F. W., Dutta, D., & Kim, S. (2017).
796 Flood inundation modelling: A review of methods, recent advances and

- 797 uncertainty analysis. *Environmental Modelling & Software*, 90, 201–216.
798 <https://doi.org/10.1016/J.ENVSOFT.2017.01.006>
- 799 UNISDR. (2011). *Global Assessment Report on Disaster Risk Reduction 2011,*
800 *Revealing Risk, Redefining Development, United Nations International Strategy*
801 *for Disaster Reduction Secretariat, Geneva, 2011.*
802 https://www.undp.org/publications/2011-global-assessment-report-disaster-risk-reduction?utm_source=EN&utm_medium=GSR&utm_content=US_UNDP_PaidSearch_Brand_English&utm_campaign=CENTRAL&c_src=CENTRAL&c_src2=GSR&gclid=CjwKCAiAqaWdBhAvEiwAGAQIttbTEIs1543d8ZuHyzCatyJutiZP2w2Wp41vZBSiouchJ7PvGplcUBoCxOYQAvD_BwE
- 803
804
805
806
- 807 UNISDR. (2013). *Global Assessment Report on Disaster Risk Reduction 2013, From*
808 *Shared Risk to Shared Value: the Business Case for Disaster Risk Reduction,*
809 *United Nations International Strategy for Disaster Reduction Secretariat,*
810 *Geneva, 2013.* <https://www.undrr.org/publication/global-assessment-report-disaster-risk-reduction-2013>
811
- 812 [van der Knijff, J. M., Younis, J., & de Roo, A. P. J. \(2010\). LISFLOOD: a GIS-based distributed](https://doi.org/10.1080/13658810802549154)
813 [model for river basin scale water balance and flood simulation. *International Journal of*](https://doi.org/10.1080/13658810802549154)
814 [*Geographical Information Science*, 24\(2\), 189–212.](https://doi.org/10.1080/13658810802549154)
815 <https://doi.org/10.1080/13658810802549154>
- 816 Varis, O., Taka, M., & Tortajada, C. (2022). Global human exposure to urban riverine
817 floods and storms. *River*. <https://doi.org/10.1002/rvr2.1>
- 818 Vu, D. T., Dang, T. D., Galelli, S., & Hossain, F. (2022). Satellite observations reveal
819 13 years of reservoir filling strategies, operating rules, and hydrological
820 alterations in the Upper Mekong River basin. *Hydrology and Earth System*
821 *Sciences*, 26(9), 2345–2364. <https://doi.org/10.5194/hess-26-2345-2022>
- 822 Ward, P. J., Jongman, B., Weiland, F. S., Bouwman, A., Van Beek, R., Bierkens, M.
823 F. P., Ligtoet, W., & Winsemius, H. C. (2013). Assessing flood risk at the
824 global scale: Model setup, results, and sensitivity. *Environmental Research*
825 *Letters*, 8(4). <https://doi.org/10.1088/1748-9326/8/4/044019>
- 826 Winsemius, H. C., Jongman, B., Veldkamp, T. I. E., Hallegatte, S., Bangalore, M., &
827 Ward, P. J. (2018). Disaster risk, climate change, and poverty: Assessing the
828 global exposure of poor people to floods and droughts. *Environment and*
829 *Development Economics*, 23(3), 328–348.
830 <https://doi.org/10.1017/S1355770X17000444>
- 831 Winsemius, H. C., van Beek, L. P. H., Jongman, B., Ward, P. J., & Bouwman, A.
832 (2013). A framework for global river flood risk assessments. *Hydrology and*
833 *Earth System Sciences*, 17(5), 1871–1892. [https://doi.org/10.5194/hess-17-](https://doi.org/10.5194/hess-17-1871-2013)
834 [1871-2013](https://doi.org/10.5194/hess-17-1871-2013)
- 835 Yamazaki, D., De Almeida, G. A. M., & Bates, P. D. (2013). Improving
836 computational efficiency in global river models by implementing the local

837 inertial flow equation and a vector-based river network map. *Water Resources*
838 *Research*, 49(11), 7221–7235. <https://doi.org/10.1002/wrcr.20552>

839 Yamazaki, D., Kanae, S., Kim, H., & Oki, T. (2011). *A physically based description*
840 *of floodplain inundation dynamics in a global river routing model.*
841 47(February), 1–21. <https://doi.org/10.1029/2010WR009726>

842 Yamazaki, D., Watanabe, S., & Hirabayashi, Y. (2018a). Global Flood Risk
843 Modeling and Projections of Climate Change Impacts. *Global Flood Hazard:*
844 *Applications in Modeling, Mapping, and Forecasting*, 233, 185–203.
845 <http://cmip-pcmdi.llnl.gov/>

846 [Yamazaki, D., Watanabe, S., & Hirabayashi, Y. \(2018b\). Global Flood Risk Modeling and](#)
847 [Projections of Climate Change Impacts. *Geophysical Monograph Series*, 233, 185–203.](#)
848 <https://doi.org/10.1002/9781119217886.CH11>

849 Yang, T., Sun, F., Gentine, P., Liu, W., Wang, H., Yin, J., Du, M., & Liu, C. (2019).
850 Evaluation and machine learning improvement of global hydrological model-
851 based flood simulations. *Environmental Research Letters*, 14(11).
852 <https://doi.org/10.1088/1748-9326/ab4d5e>

853 [Yoshida, T., Hanasaki, N., Nishina, K., Boulange, J., Okada, M., & Troch, P. A. \(2022\).](#)
854 [Inference of Parameters for a Global Hydrological Model: Identifiability and Predictive](#)
855 [Uncertainties of Climate-Based Parameters. *Water Resources Research*, 58\(2\),](#)
856 [e2021WR030660. https://doi.org/10.1029/2021WR030660](https://doi.org/10.1029/2021WR030660)

857 Zajac, Z., Revilla-Romero, B., Salamon, P., Burek, P., Hirpa, F., & Beck, H. (2017).
858 The impact of lake and reservoir parameterization on global streamflow
859 simulation. *Journal of Hydrology*, 548, 552–568.
860 <https://doi.org/10.1016/j.jhydrol.2017.03.022>

861 Zhao, F., Veldkamp, T. I. E., Frieler, K., Schewe, J., Ostberg, S., Willner, S.,
862 Schauburger, B., Gosling, S. N., Schmied, H. M., Portmann, F. T., Leng, G.,
863 Huang, M., Liu, X., Tang, Q., Hanasaki, N., Biemans, H., Gerten, D., Satoh, Y.,
864 Pokhrel, Y., ... Yamazaki, D. (2017). The critical role of the routing scheme in
865 simulating peak river discharge in global hydrological models. *Environmental*
866 *Research Letters*, 12(7). <https://doi.org/10.1088/1748-9326/aa7250>

867 **Formatted:** Indent: Left: -0.06 cm, First line: 0 cm

Deleted: 2018

Page 2: [1] Formatted Vimal Mishra 04/12/2023 09:37:00

Font: Times New Roman

Page 2: [2] Formatted Vimal Mishra 04/12/2023 09:37:00

Font: Times New Roman

Page 2: [3] Formatted Vimal Mishra 04/12/2023 09:37:00

Font: Times New Roman

Page 2: [3] Formatted Vimal Mishra 04/12/2023 09:37:00

Font: Times New Roman

Page 2: [3] Formatted Vimal Mishra 04/12/2023 09:37:00

Font: Times New Roman

Page 2: [4] Formatted Vimal Mishra 04/12/2023 09:37:00

Font: Times New Roman

Page 2: [5] Formatted Vimal Mishra 04/12/2023 09:37:00

Font: Times New Roman

Page 2: [5] Formatted Vimal Mishra 04/12/2023 09:37:00

Font: Times New Roman

Page 2: [5] Formatted Vimal Mishra 04/12/2023 09:37:00

Font: Times New Roman

Page 2: [6] Formatted Vimal Mishra 04/12/2023 09:37:00

Font: Times New Roman

Page 2: [7] Formatted Vimal Mishra 04/12/2023 09:37:00

Font: Times New Roman

Page 2: [7] Formatted Vimal Mishra 04/12/2023 09:37:00

Font: Times New Roman

Page 2: [8] Formatted Vimal Mishra 04/12/2023 09:37:00

Font: Times New Roman

Page 2: [9] Formatted Vimal Mishra 04/12/2023 09:37:00

Font: Times New Roman

Page 2: [9] Formatted Vimal Mishra 04/12/2023 09:37:00

Font: Times New Roman

Page 2: [9] Formatted Vimal Mishra 04/12/2023 09:37:00

Font: Times New Roman

Page 2: [9] Formatted Vimal Mishra 04/12/2023 09:37:00

Font: Times New Roman

Page 2: [10] Formatted Vimal Mishra 04/12/2023 09:37:00

Font: Times New Roman

Page 2: [10] Formatted Vimal Mishra 04/12/2023 09:37:00

Font: Times New Roman

Page 2: [10] Formatted Vimal Mishra 04/12/2023 09:37:00

Font: Times New Roman

Page 2: [10] Formatted Vimal Mishra 04/12/2023 09:37:00

Font: Times New Roman

Page 2: [11] Formatted Vimal Mishra 04/12/2023 09:37:00

Font: Times New Roman

Page 2: [12] Formatted Vimal Mishra 04/12/2023 09:37:00

Font: Times New Roman

Page 2: [12] Formatted Vimal Mishra 04/12/2023 09:37:00

Font: Times New Roman

Page 2: [12] Formatted Vimal Mishra 04/12/2023 09:37:00

Font: Times New Roman

Page 2: [13] Formatted Vimal Mishra 04/12/2023 09:37:00

Font: Times New Roman

Page 2: [14] Formatted Vimal Mishra 04/12/2023 09:37:00

Font: Times New Roman

Page 2: [14] Formatted Vimal Mishra 04/12/2023 09:37:00

Font: Times New Roman

Page 2: [14] Formatted Vimal Mishra 04/12/2023 09:37:00

Font: Times New Roman

Page 2: [15] Formatted Vimal Mishra 04/12/2023 09:37:00

Font: Times New Roman

Page 2: [16] Formatted Vimal Mishra 04/12/2023 09:37:00

Font: Times New Roman

Page 2: [16] Formatted Vimal Mishra 04/12/2023 09:37:00

Font: Times New Roman

Page 2: [16] Formatted Vimal Mishra 04/12/2023 09:37:00

Font: Times New Roman

Page 2: [17] Formatted Vimal Mishra 04/12/2023 09:37:00

Font: Times New Roman, 10 pt

Page 2: [18] Formatted Vimal Mishra 04/12/2023 09:37:00

Font: Times New Roman

Page 2: [18] Formatted Vimal Mishra 04/12/2023 09:37:00

Font: Times New Roman

Page 2: [19] Formatted Vimal Mishra 04/12/2023 09:37:00

Font: Times New Roman

Page 2: [20] Formatted Vimal Mishra 04/12/2023 09:37:00

Font: Times New Roman

Page 2: [21] Formatted Vimal Mishra 04/12/2023 09:37:00

Font: Times New Roman

Page 2: [21] Formatted Vimal Mishra 04/12/2023 09:37:00

Font: Times New Roman

Page 2: [21] Formatted Vimal Mishra 04/12/2023 09:37:00

Font: Times New Roman

Page 2: [22] Formatted Vimal Mishra 04/12/2023 09:37:00

Font: Times New Roman

Page 2: [23] Formatted Vimal Mishra 04/12/2023 09:37:00

Font: Times New Roman

Page 2: [23] Formatted Vimal Mishra 04/12/2023 09:37:00

Font: Times New Roman

Page 2: [23] Formatted Vimal Mishra 04/12/2023 09:37:00

Font: Times New Roman

Page 2: [24] Formatted Vimal Mishra 04/12/2023 09:37:00

Font: Times New Roman, 10 pt

Page 2: [25] Formatted Vimal Mishra 04/12/2023 09:37:00

Font: Times New Roman

Page 2: [25] Formatted Vimal Mishra 04/12/2023 09:37:00

Font: Times New Roman

Page 2: [25] Formatted Vimal Mishra 04/12/2023 09:37:00

Font: Times New Roman

Page 2: [26] Formatted Vimal Mishra 04/12/2023 09:37:00

Font: Times New Roman

Page 2: [26] Formatted Vimal Mishra 04/12/2023 09:37:00

Font: Times New Roman

Page 2: [26] Formatted Vimal Mishra 04/12/2023 09:37:00

Font: Times New Roman

Page 2: [27] Formatted Vimal Mishra 04/12/2023 09:37:00

Font: Times New Roman

Page 2: [28] Formatted Vimal Mishra 04/12/2023 09:37:00

Font: Times New Roman

Page 2: [28] Formatted Vimal Mishra 04/12/2023 09:37:00

Font: Times New Roman

Page 2: [29] Formatted Vimal Mishra 04/12/2023 09:37:00

Font: Times New Roman

Page 2: [30] Formatted Vimal Mishra 04/12/2023 09:37:00

Font: Times New Roman

Page 2: [30] Formatted Vimal Mishra 04/12/2023 09:37:00

Font: Times New Roman

Page 2: [30] Formatted Vimal Mishra 04/12/2023 09:37:00

Font: Times New Roman

Page 2: [31] Formatted Vimal Mishra 04/12/2023 09:37:00

Font: Times New Roman, 10 pt

Page 2: [32] Formatted Vimal Mishra 04/12/2023 09:37:00

Font: Times New Roman

Page 2: [32] Formatted Vimal Mishra 04/12/2023 09:37:00

Font: Times New Roman

Page 2: [32] Formatted Vimal Mishra 04/12/2023 09:37:00

Font: Times New Roman

Page 2: [33] Formatted Vimal Mishra 04/12/2023 09:37:00

Font: Times New Roman

Page 2: [33] Formatted Vimal Mishra 04/12/2023 09:37:00

Font: Times New Roman

Page 2: [33] Formatted Vimal Mishra 04/12/2023 09:37:00

Font: Times New Roman

Page 2: [34] Formatted Vimal Mishra 04/12/2023 09:37:00

Font: Times New Roman

Page 2: [35] Formatted Vimal Mishra 04/12/2023 09:37:00

Font: Times New Roman

Page 2: [36] Formatted Vimal Mishra 04/12/2023 09:37:00

Font: Times New Roman

Page 2: [36] Formatted Vimal Mishra 04/12/2023 09:37:00

Font: Times New Roman

Page 2: [37] Formatted Vimal Mishra 04/12/2023 09:37:00

Font: Times New Roman

Page 2: [38] Formatted Vimal Mishra 04/12/2023 09:37:00

Font: Times New Roman

Page 2: [39] Formatted Vimal Mishra 04/12/2023 09:37:00

Font: Times New Roman

Page 2: [39] Formatted Vimal Mishra 04/12/2023 09:37:00

Font: Times New Roman

Page 2: [40] Formatted Vimal Mishra 04/12/2023 09:37:00

Font: Times New Roman

Page 2: [41] Formatted Vimal Mishra 04/12/2023 09:37:00

Font: Times New Roman

Page 2: [42] Formatted Vimal Mishra 04/12/2023 09:37:00

Font: Times New Roman

Page 2: [42] Formatted Vimal Mishra 04/12/2023 09:37:00

Font: Times New Roman

Page 2: [43] Formatted Vimal Mishra 04/12/2023 09:37:00

Font: Times New Roman

Page 2: [44] Formatted Vimal Mishra 04/12/2023 09:37:00

Font: Times New Roman, 10 pt, Font colour: Black

Page 2: [45] Formatted Vimal Mishra 04/12/2023 09:37:00

Font: Times New Roman

Page 2: [45] Formatted Vimal Mishra 04/12/2023 09:37:00

Font: Times New Roman

Page 3: [46] Formatted Vimal Mishra 04/12/2023 09:37:00

Font: Times New Roman

Page 3: [47] Formatted Vimal Mishra 04/12/2023 09:37:00

Font: Times New Roman

Page 3: [48] Formatted Vimal Mishra 04/12/2023 09:37:00

Font: Times New Roman

Page 3: [49] Formatted Vimal Mishra 04/12/2023 09:37:00

Font: Times New Roman

Page 3: [50] Formatted Vimal Mishra 04/12/2023 09:37:00

Font: Times New Roman

Page 3: [51] Formatted Vimal Mishra 04/12/2023 09:37:00

Font: Times New Roman

Page 3: [52] Formatted Vimal Mishra 04/12/2023 09:37:00

Font: Times New Roman

Page 3: [53] Formatted Vimal Mishra 04/12/2023 09:37:00

Font: Times New Roman

Page 3: [54] Formatted Vimal Mishra 04/12/2023 09:37:00

Font: Times New Roman

Page 3: [55] Formatted Vimal Mishra 04/12/2023 09:37:00

Font: Times New Roman

Page 3: [56] Formatted Vimal Mishra 04/12/2023 09:37:00

Font: Times New Roman

Page 3: [57] Formatted Vimal Mishra 04/12/2023 09:37:00

Font: Times New Roman

Page 3: [58] Formatted Vimal Mishra 04/12/2023 09:37:00

Font: Times New Roman

Page 3: [59] Formatted Vimal Mishra 04/12/2023 09:37:00

Font: Times New Roman

Page 3: [60] Formatted Vimal Mishra 04/12/2023 09:37:00

Font: Times New Roman

Page 3: [61] Formatted Vimal Mishra 04/12/2023 09:37:00

Font: Times New Roman

Page 3: [62] Formatted Vimal Mishra 04/12/2023 09:37:00

Font: Times New Roman

Page 3: [63] Formatted Vimal Mishra 04/12/2023 09:37:00

Font: Times New Roman

Page 3: [64] Formatted Vimal Mishra 04/12/2023 09:37:00

Font: Times New Roman

Page 3: [65] Formatted Vimal Mishra 04/12/2023 09:37:00

Font: Times New Roman

Page 3: [66] Formatted Vimal Mishra 04/12/2023 09:37:00

Font: Times New Roman, 10 pt

Page 3: [67] Formatted Vimal Mishra 04/12/2023 09:37:00

Font: Times New Roman

Page 3: [68] Formatted Vimal Mishra 04/12/2023 09:37:00

Font: Times New Roman

Page 3: [69] Formatted Vimal Mishra 04/12/2023 09:37:00

Font: Times New Roman

Page 3: [70] Formatted Vimal Mishra 04/12/2023 09:37:00

Font: Times New Roman

Page 3: [71] Formatted Vimal Mishra 04/12/2023 09:37:00

Font: Times New Roman

Page 3: [72] Formatted Vimal Mishra 04/12/2023 09:37:00

Font: Times New Roman

Page 3: [73] Formatted Vimal Mishra 04/12/2023 09:37:00

Font: Times New Roman

Page 3: [74] Formatted Vimal Mishra 04/12/2023 09:37:00

Font: Times New Roman

Page 3: [75] Formatted Vimal Mishra 04/12/2023 09:37:00

Font: Times New Roman

Page 3: [76] Formatted Vimal Mishra 04/12/2023 09:37:00

Font: Times New Roman

Page 3: [77] Formatted Vimal Mishra 04/12/2023 09:37:00

Font: Times New Roman

Page 3: [78] Formatted Vimal Mishra 04/12/2023 09:37:00

Font: Times New Roman

Page 3: [79] Formatted Vimal Mishra 04/12/2023 09:37:00

Font: Times New Roman

Page 3: [80] Formatted Vimal Mishra 04/12/2023 09:37:00

Font: Times New Roman

Page 3: [81] Formatted Vimal Mishra 04/12/2023 09:37:00

Font: Times New Roman

Page 3: [82] Formatted Vimal Mishra 04/12/2023 09:37:00

Font: Times New Roman, 10 pt

Page 3: [83] Formatted Vimal Mishra 04/12/2023 09:37:00

Font: Times New Roman

Page 3: [84] Formatted Vimal Mishra 04/12/2023 09:37:00

Font: Times New Roman

Page 3: [85] Formatted Vimal Mishra 04/12/2023 09:37:00

Font: Times New Roman

Page 3: [86] Formatted Vimal Mishra 04/12/2023 09:37:00

Font: Times New Roman

Page 3: [87] Formatted Vimal Mishra 04/12/2023 09:37:00

Font: Times New Roman

Page 3: [88] Formatted Vimal Mishra 04/12/2023 09:37:00

Font: Times New Roman

Page 3: [89] Formatted Vimal Mishra 04/12/2023 09:37:00

Font: Times New Roman

Page 3: [90] Formatted Vimal Mishra 04/12/2023 09:37:00

Font: Times New Roman